



**Dynamiques saisonnières de la méthanotrophie et des gaz à effet de serre
dans un lac boréal**

par Noémie Gaudreault

**Mémoire présenté à l'Université du Québec à Chicoutimi en vue de l'obtention du grade
de Maître ès sciences (M. Sc.) en ressources renouvelables**

Québec, Canada

© Noémie Gaudreault, 2024

Résumé

Le couvert de glace hivernal empêche les gaz à effet de serre (GES) de s'échapper d'un lac, les emprisonnant sous et dans la glace. La quantité de gaz qui sera libérée au moment de la fonte de la glace dépend de l'activité microbienne et des conditions environnementales sous la glace pendant l'hiver. Les méthanotrophes joueraient un rôle crucial en limitant les émissions de CH₄ des sédiments anoxiques vers l'atmosphère, mais on en sait peu sur leur dynamique saisonnière ou leur réponse aux changements de durée du couvert de glace et de régime d'oxygène hivernal. Alors que les conditions hypoxiques sous la glace peuvent ralentir le métabolisme microbien aérobie, le piégeage du CH₄ sous la glace empêchant sa diffusion dans l'atmosphère peut permettre aux méthanotrophes de le métaboliser pendant des périodes plus longues – la durée du couvert de glace peut donc favoriser l'oxydation du CH₄. Nous présentons les variations saisonnières sur 9 mois des organismes microbiens, notamment la diversité et l'abondance des méthanotrophes avec le séquençage de l'ARNr 16S et l'expression du gène codant pour leur capacité d'oxydation du CH₄ (*pmoA*) par RT-qPCR, ainsi que du CH₄ et du CO₂ dissous, où nous avons exploré leur accumulation sous la glace et leurs émissions printanières. Nous avons observé que les concentrations de CH₄ et d'azote total étaient des facteurs déterminants de l'activité méthanotrophe, qui était plus prononcée dans des conditions pauvres en oxygène au plus profond du lac et au printemps. Des variations saisonnières entre les genres de méthanotrophes ont également été détectées, notamment pour *Methylobacter* qui a augmenté et *Candidatus Methyloacidiphilum* qui a diminué pendant la période hivernale. Des signes de méthanotrophie ont également été détectés dans la glace du lac. Cette étude contribue aux études hivernales sur le cycle du CH₄ dans les lacs boréaux et approfondit notre compréhension des conséquences des hivers plus courts et plus chauds sur le cycle du carbone des lacs en reliant le couvert de glace et les régimes d'oxygène à la méthanotrophie.

Abstract

Winter ice cover prevents greenhouse gases (GHG) from escaping a lake, trapping them under and in the ice. The quantity of gases that will be released at the ice-off depends on the microbial activity and environmental conditions under the ice during winter. Methanotrophs are thought to play a crucial role in limiting CH₄ emissions from the anoxic sediments into the water column and subsequently to the atmosphere, yet little is known about their seasonal dynamics or how they will respond to ice cover duration and winter oxygen regimes. While hypoxic conditions under ice may slow microbial aerobic metabolism, the trapping of CH₄ under ice preventing its diffusion into the atmosphere may allow for longer periods of time for methanotrophs to metabolize it – duration of ice may therefore control CH₄ oxidation. We present seasonal variations over 9 months of microbial organisms, including the diversity and abundance of methanotrophs with 16S rRNA sequencing and expression of the gene encoding their methane-oxidization capability (*pmoA*) using RT-qPCR, and of dissolved CH₄ and CO₂, where we explored under ice accumulation and spring emissions. We found that CH₄ and total nitrogen concentrations were drivers of methanotrophic activity which was most pronounced in oxygen-depleted conditions at the deepest water depths and in spring. Seasonal variations among methanotroph genera were also present, notably for *Methylobacter* that increased and *Candidatus Methylacidiphilum* that decreased in the winter period. Signs of methanotrophy were also found in the lake ice. This study contributes to winter lake studies on the CH₄ cycle in boreal settings and furthers our understanding of the consequences of shorter and warmer winters on lake carbon cycling by linking ice cover and oxygen regimes to methanotrophy.

Table des matières

Résumé	ii
Abstract	ii
Liste des tableaux	iv
Liste des figures.....	v
Liste des abréviations	vi
Remerciements	vii
Contexte de l'étude et plan du mémoire.....	viii
CHAPITRE 1: Introduction générale.....	1
1.1 Introduction.....	1
1.1.1 L'importance des lacs dans le cycle du carbone.....	1
1.1.2 La stratification verticale des lacs et la saisonnalité.....	2
1.1.3 Rôle des microorganismes dans le cycle aquatique du carbone	4
1.1.4 Les méthanogènes.....	5
1.1.5 Les méthanotrophes	6
1.1.6 La portée de la limnologie hivernale	7
1.1.7 Objectifs.....	10
1.2 Méthodologie	10
CHAPITRE 2: Methanotrophy throughout winter and shoulder seasons in a boreal lake.....	14
2.1 Introduction.....	14
2.2 Materials and methods	17
2.2.1 Study site	17
2.2.2 Sampling design.....	18
2.2.3 Sampling processing.....	20
2.2.4 Nucleic acid extraction	21
2.2.5 Sequencing and read processing.....	22
2.2.6 Quantitative PCR gene quantification	23
2.2.7 Statistical analyses	24
2.2.8 Data availability.....	25
2.3 Results.....	26
2.4 Discussion	34
2.4.1 Ice cover impacted Lake Simoncouche limnology.....	34
2.4.2 Microbial communities varied under ice	37
2.4.3 Negligible CH ₄ concentrations in winter.....	40
2.4.4 Methanotrophy in hypoxic zones and spring peak	42
2.4.5 CH ₄ and TN as drivers of methanotrophic activity.....	44
2.4.6 Methanotrophy in lake ice	46
2.4.7 Conclusion	47
CHAPITRE 3 : Conclusion générale.....	48
Liste de références.....	52
ANNEXES	63

Liste des tableaux

Table 1 Concentration of total nitrogen (TN), total phosphorus (TP), dissolved organic carbon (DOC) and spectral indices such as specific UV absorbance (SUVA), spectral slope at 285 nm (S285) and absorbance coefficient at 440 (a440) of CDOM. For variables with replicated samples, average values are provided together with standard deviation.	28
---	----

Liste des figures

Figure 1 Stratification saisonnière d'un lac boréal dimictique typique A) en été, B) en automne, C) en hiver et D) au printemps, la température étant représentée en bleu et l'oxygène en rouge.	3
Figure 2 Sources de méthane et d'oxygène dans un lac boréal en été et en hiver, adapté de Li et Xue (2021) sous licence CC BY.	8
Figure 3 A) Location of Lake Simoncouche in Quebec, Canada (green point) and B) bathymetric map of Lake Simoncouche. The red point represents z_{\max} . The map of Canada is from © Creative Commons under the license Attribution-Share Alike 4.0 International, the points and coordinates were added.	18
Figure 4 A) Ice and snow thickness over the sampling period. B) Dissolved oxygen (DO) (red) and temperature (blue) in the vertical column of the lake in fall (22 September, 20 October, 01 December), early winter (19 December, 19 January), late winter (15 February, 15 March, 14 April) and spring (27 April and 24 May). Within each season, months are identified by their first letter and colored from darker to lighter hues over time.	27
Figure 5 A) NMDS of Bray-Curtis dissimilarity of microbial communities of Lake Simoncouche represented by their habitat (water, sediments and ice) and sampling date, and with lines connecting biological replicates. B) Alpha diversity represented by the Shannon index for each habitat over time.	30
Figure 6 Relative abundance of methanotroph genera in duplicate samples based on sequencing of the 16S rRNA gene in A) the ice, B) 0 m water, C) 3 m water, D) 7 m water and E) sediments. Note different scales used across habitats. The dates on the x-axis are colored according to seasons. Low abundance genera were grouped in "Others", and include <i>Methylomonas</i> , <i>Methylosphaera</i> , <i>Methyloterricola</i> , <i>Methylovulum</i> , <i>Methyloglobulus</i> , <i>Methylosinus</i> , <i>Methylosoma</i> , <i>Candidatus Methylospira</i> and <i>Methylomagnum</i> .	31
Figure 7 Dissolved CH ₄ concentrations in A) the water column and B) the sediments; dissolved CO ₂ concentrations in C) the water column and D) the sediments; and E) copy number of <i>pmoA</i> transcripts, every dot being a technical replicate (6 total per sample). *Original value at $103.25 \pm 17.7 \mu\text{M}$, cut for visibility.	33
Figure 8 Relative importance weights (%) of A) environmental variables, and methanotrophic genera in B) the water column and C) sediments explaining copy numbers of the <i>pmoA</i> gene. The (-) indicates a negative relationship between the variables and the activity. C. stands for candidatus.	34

Liste des abréviations

ADNc	ADN complémentaire
AIC	<i>Akaike information criterion</i> (critère d'information d'Akaike)
ASL	<i>Above sea level</i> (au-dessus du niveau de la mer)
ASV	<i>Amplicon sequence variant</i> (variant de séquence d'amplicon)
a ₄₄₀	Coefficient d'absorption à 440 nm
C.	<i>Candidatus</i>
CH ₄	Méthane
CO ₂	Dioxyde de carbone
CDOM	<i>Colored dissolved organic matter</i> (matière organique dissoute colorée)
Cq	Cycle de quantification
DO	<i>Dissolved oxygen</i> (oxygène dissous)
DOC	<i>Dissolved organic carbon</i> (carbone organique dissous)
F / R	<i>Forward / Reverse</i> (Sens / Anti-sens)
GES (Fr) / GHG (Ang)	Gaz à effet de serre / <i>Greenhouse gases</i>
LPSN	<i>List of Prokaryotic names with Standing in Nomenclature</i>
MCR	Méthyl-coenzyme M réductase
MOB	<i>Methane oxidizing bacteria</i> (bactéries oxydant le méthane)
NMDS	<i>Non-metric multidimensional scaling</i> (positionnement multidimensionnel non-métrique)
NTC	<i>No template control</i> (contrôle négatif)
pb (Fr) / bp (Ang)	Paire de bases / <i>base pair</i>
pMMO / sMMO	<i>Particulate methane monoxygenase / soluble</i> (méthane monoxygénase particulaire / soluble)
PCR	<i>Polymerase chain reaction</i> (réaction en chaîne par polymérase)
qPCR	<i>Quantitative polymerase chain reaction</i> (réaction en chaîne par polymérase quantitative)
RVI	<i>Relative variable importance</i> (importance relative des variables)
S ₂₈₅	Pente spectrale à 285 nm
SQ	<i>Starting quantity</i> (quantité initiale)
SRA	<i>Sequence Read Archive</i>
SUVA	<i>Specific UV absorbance</i> / Absorbance-UV spécifique (254 nm)
TN	<i>Total nitrogen</i> (azote total)
TP	<i>Total phosphorus</i> (phosphore total)
Z _{max}	Profondeur maximale

Remerciements

J'adresse d'abord mes remerciements à ma directrice Catherine Girard pour m'avoir partagé le formidable monde de l'écologie microbienne, un domaine qui a su me passionner en moins de temps qu'il ne le faut pour le mentionner. Je suis également reconnaissante pour la confiance qu'elle m'a accordée ces dernières années pour contribuer à la naissance du nouveau laboratoire du Patrimoine microbien et pour les incroyables opportunités qu'elle m'a offertes et qui m'ont sortie de ma zone de confort. Merci pour tous les encouragements et tous les bons mots lors de nos rencontres hebdomadaires, moments qui ont souvent été la seule demi-heure nécessaire pour recharger toute ma motivation à avancer. Merci d'être une directrice accessible et compréhensive, qui a toujours tenté de m'amener à me dépasser plus que je ne l'aurais jamais fait moi-même. Je tiens également à remercier mes codirecteurs Milla Rautio et Vilmantas Prėskienis pour leur incroyable passion pour la recherche, pour avoir pris le temps de répondre à mes questions, pour leurs suggestions plus qu'intéressantes et pour leur désir infini d'amener ce projet le plus loin possible, même si ce n'était « qu'une seule maîtrise ».

Je veux exprimer ma gratitude aux membres du laboratoire qui ont participé à mes excursions hivernales pour l'échantillonnage de ce projet, soient Jean-Simon Boulianne, Maxime Larose, Pénélope Blackburn-Desbiens, Thanuri Kasthuri Arachchi et Mukund Gauthankar. Merci pour votre enthousiasme contagieux au point de me demander si vous pouviez participer au terrain avant même que je n'aie commencé à le préparer. Je suis profondément reconnaissante de l'aide fournie par Pierre-Luc Savard et Patrick Nadeau de la Forêt d'Enseignement et de Recherche Simoncouche pour le support sur le terrain et la coordination de nos embarcations chaque mois. Je n'aurais jamais pu accomplir cette recherche sans l'aide et l'appui en laboratoire de notre technicienne Crysta Rhains, ainsi que de Marie-Ève Lavoie, Claire Fournier, Paul George et Claude Lachance. Je tiens à envoyer un énorme merci aux membres de l'Aqualab pour leur support et leur solidité face à mes hautes émotions, particulièrement Paola Ayala Borda pour sa bienveillance et sa sagesse, ainsi que Crysta Rhains pour son oreille et ses bras ouverts.

Je souhaite également remercier les membres de mon entourage qui m'ont supportée et encouragée tout au long de ce processus, que ce soit pour célébrer mes succès parfois plus que moi (merci maman) ou dans les abysses où j'avais besoin d'encouragements. Merci à mon merveilleux Simon de m'avoir involontairement imposé un horaire de vie plus sain en m'interdisant de m'asseoir à mon bureau lors des fins de semaine. Merci à Mylène Gagnon d'exister, car elle sait toujours sur quelle longueur d'onde me retrouver et quels *memes* m'envoyer. Je veux également remercier mon frère Simon Lalancette pour son aide (qui ne vient jamais sans moqueries) vis-à-vis mes talents dans R.

Plus formellement, j'aimerais souligner le support financier du Conseil de recherches en sciences naturelles et en génie du Canada (CRSNG), du Fonds de Recherche du Québec – Nature et Technologie (FRQNT) (subvention 330476) et du Groupe de recherche interuniversitaire en limnologie (GRIL).

Contexte de l'étude et plan du mémoire

Les microorganismes ont longtemps été la seule forme de vie sur Terre. Ils ont transformé l'évolution de la vie, tout en étant des moteurs essentiels pour nos écosystèmes. Depuis les premières observations de microorganismes et de cellules au 17^e siècle, la microbiologie s'est bien développée : en passant des pommes de terre aux géloses pour les mettre en culture, la communauté scientifique a usé de son imaginaire collectif pour isoler ces organismes afin de mieux en comprendre les rôles. De nouvelles technologies en biologie moléculaire ont toutefois permis de découvrir que nombreux sont les microorganismes dans l'environnement qui demeurent toujours impossibles à mettre en culture en laboratoire. Le séquençage métagénomique, où l'idée est de collecter les acides nucléiques directement dans l'environnement et de cibler les gènes d'intérêt, est propulsé par les nouvelles techniques de séquençage et de qPCR, ce qui a révolutionné le domaine de l'écologie microbienne. Dans ce mémoire, il est question d'utiliser ces techniques pour étudier la présence et l'activité de microorganismes impliqués dans le cycle lacustre du méthane en hiver, une saison sous-étudiée bien qu'elle représente près de la moitié de l'année en zone boréale. En vue des changements importants dans le régime hivernal dû au réchauffement climatique, les techniques moléculaires représentent une approche puissante pour comprendre les conséquences et appréhender le futur de nos écosystèmes.

Le premier chapitre de ce mémoire de maîtrise est une introduction générale aux lacs boréaux et leur stratification saisonnière, aux microorganismes impliqués dans le cycle lacustre du méthane, ainsi qu'à l'importance des études limnologiques hivernales, particulièrement dans le contexte du réchauffement climatique. La section se termine sur les objectifs de la recherche ainsi que sur une brève présentation de la méthodologie. Le second chapitre est présenté sous forme d'article scientifique rédigé en anglais intitulé « Methanotrophy throughout winter and shoulder seasons in a boreal lake » avec Vilmantas Prėskienis, Milla Rautio et Catherine Girard comme coauteurs. Cet article est en préparation et sera soumis pour révision par les pairs au journal *Limnology & Oceanography* (ASLO). Il présente la méthodologie complète, les résultats de la recherche ainsi que leur discussion. Le troisième et dernier chapitre est une conclusion générale de la recherche résumant les résultats principaux et proposant des pistes de recherche futures.

CHAPITRE 1: Introduction générale

1.1 Introduction

1.1.1 L'importance des lacs dans le cycle du carbone

La région boréale est un des biomes ayant la plus forte densité de lacs, ceux-ci représentant au moins 10% de son territoire (Rasilo *et al.* 2015), et le Québec à lui seul compte au moins 600 000 lacs (Boyce 2006). Les lacs se situent aux points les plus bas dans le paysage, ce qui leur permet d'agir comme intégrateurs de changements dans leurs bassins versants (Linz *et al.* 2018; Vincent 2019). Les apports du territoire environnant peuvent en effet altérer leurs propriétés physique, chimique et biologique, ce qui confère un rôle de sentinelle aux lacs (Williamson *et al.* 2009; Linz *et al.* 2018). Parallèlement, les lacs boréaux jouent un rôle considérable dans le cycle du carbone : ils servent au stockage, au traitement et à la production de gaz à effet de serre (GES) tels que le dioxyde de carbone (CO₂) et le méthane (CH₄), qui peuvent ensuite être relâchés dans l'atmosphère par diffusion et ébullition (Cole *et al.* 2007; Williamson *et al.* 2009; Rasilo *et al.* 2015). Ces gaz sont impliqués dans les changements climatiques puisqu'ils absorbent la radiation dans l'atmosphère et y retiennent la chaleur. Ils s'accumulent dans l'atmosphère plus rapidement que leur carbone n'est séquestré dans les sols, les océans ou les organismes vivants, menant à un réchauffement atmosphérique progressif. Le CO₂ est le gaz contribuant le plus au réchauffement, étant responsable de 66% du forçage radiatif (concentration atmosphérique de 420 ppm en 2022), suivi du CH₄ qui en est responsable à 16% (2 ppm en 2022). (Gouvernement du Canada 2023). Bien que le CH₄ soit moins abondant, son potentiel de réchauffement pour le même poids est 30 fois plus élevé que le CO₂ (Borrel *et al.* 2011; Samad et Bertilsson 2017).

1.1.2 La stratification verticale des lacs et la saisonnalité

La plupart des lacs ont des couches d'eau aux propriétés diverses en fonction de leur profondeur, en raison des propriétés de densité et de température de l'eau (Jones et Smol 2023). La densité de l'eau est maximale à 4 °C (Vincent 2019). Ainsi, en été, l'eau de surface d'un lac approche la température de l'atmosphère, tandis que le fond du lac est à une température de 4 °C. La couche supérieure du lac est appelée l'épilimnion, tandis que la couche du fond est l'hypolimnion (Figure 1A). Le gradient de température au sein de la colonne d'eau n'est pas graduel : ces valeurs changent drastiquement au niveau de la thermocline. Celle-ci est la troisième couche d'eau d'un lac et elle sépare l'épilimnion de l'hypolimnion, tout limitant les échanges entre les deux couches en raison de la forte différence de densité (Jones et Smol 2023) (Figure 1A). L'oxygène, un élément nécessaire à la survie de la majorité des organismes, est une autre variable qui subit un important changement à la thermocline du lac puisque sa solubilité dépend de la température. Deux grandes sources contribuent à l'apport d'oxygène au sein d'un lac : la diffusion de l'atmosphère vers l'eau, aidée par le brassage de l'épilimnion par les vents; puis la production primaire par les organismes photosynthétiques aquatiques dans les zones où la pénétration de la lumière est suffisante (Jones et Smol 2023). L'épilimnion, en raison de sa proximité avec l'atmosphère et de son régime lumineux plus important, est donc riche en oxygène, tandis que l'hypolimnion, isolé de la surface et recevant peu de lumière puisqu'elle s'atténue avec la profondeur, peut atteindre un taux d'oxygène limitant la survie des organismes (hypoxie). En contrepartie, l'oxygène est consommé par les organismes vivants tels que les animaux, les végétaux et les microorganismes aquatiques.

En région boréale, à l'automne, les températures chutent et la durée du jour diminue, ce qui impacte la température de l'épilimnion qui suit celle de l'atmosphère. Avec une diminution de la température de l'eau vient une augmentation de la densité, favorisant sa plongée dans la colonne d'eau et amorçant le processus du brassage (Figure 1B), aidé par les vents forts de

l'automne (Vincent 2019). Ainsi, l'eau à la surface du lac coule vers le fond dans une circulation convective qui homogénéise éventuellement l'entièreté de la colonne d'eau en ce qui concerne la température, mais aussi l'oxygène, les nutriments, le CO₂, le CH₄ et d'autres particules qui y sont entraînés (Jones et Smol 2023). Le brassage de la colonne d'eau survient deux fois par année (automne et printemps) dans la majorité des lacs boréaux – on les qualifie donc de lacs dimictiques (Jones et Smol 2023). Ce phénomène peut durer quelques semaines à l'automne, tandis qu'il surviendra en quelques jours seulement au printemps (Vincent 2019).

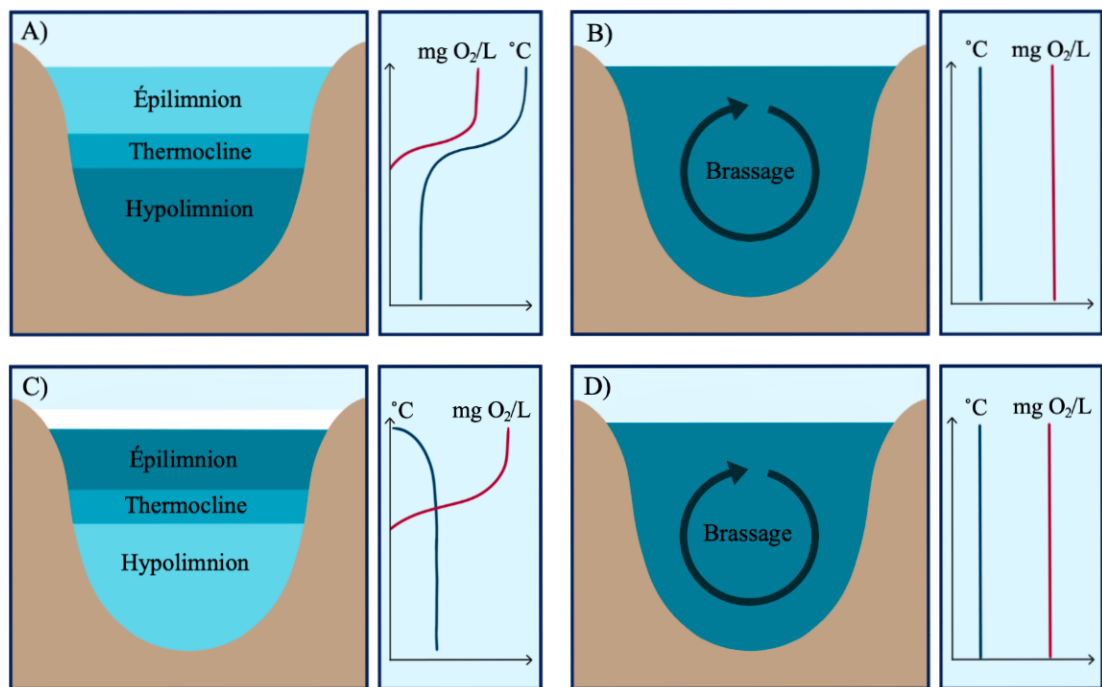


Figure 1 Stratification saisonnière d'un lac boréal dimictique typique A) en été, B) en automne, C) en hiver et D) au printemps, la température étant représentée en bleu et l'oxygène en rouge.

En hiver, on assiste à une stratification du lac qui est inversée par rapport à la saison estivale (Figure 1C), en raison de la densité maximale de l'eau à 4 °C. Ainsi, la stratification du lac est maintenant composée d'un épilimnion froid (plus près des températures atmosphériques) et d'un hypolimnion plus chaud (à 4 °C, et donc à densité maximale) (Vincent 2019). La température dans l'épilimnion est près de 0 °C et, puisque c'est le point de

congélation de l'eau douce, un couvert de glace se forme à la surface du lac. Ce phénomène se produit annuellement et dure plusieurs mois en région boréale, en plus de concerner 86% des lacs sur Terre (Korver *et al.* 2024). Le couvert de glace peut typiquement être divisé en deux types de glace, soit la glace noire et la glace blanche. La première est formée par l'eau du lac qui gèle à sa surface, elle est transparente et plus solide que la glace blanche, qui provient des cycles de gel et dégel de la neige ou de pluie accumulés sur le couvert de glace (Leppäranta 2015).

Vers la fin de l'hiver, le brassage printanier (Figure 1D) survient et apporte plusieurs changements vitaux pour le cycle des lacs dimictiques (Imrit et Sharma 2021). Avec l'augmentation de la température de l'air, la neige et le couvert de glace fondent : l'oxygène de l'atmosphère peut entrer dans l'eau du lac à nouveau grâce aux vents et à la diffusion, ainsi il n'est plus une ressource limitante (Jansen *et al.* 2021). Également, la neige du bassin versant fond et ruisselle vers le lac, entraînant une grande quantité de nutriments, de solutés, de matière organique dissoute et d'oxygène (Jansen *et al.* 2021; Jones et Smol 2023). Les eaux sont brassées avec le réchauffement qui augmente la densité de l'eau dans l'épilimnion, puis les particules et nutriments qui s'étaient déposés sur les sédiments seront remis en suspension dans la colonne d'eau. La stratification estivale s'établira relativement rapidement.

1.1.3 Rôle des microorganismes dans le cycle aquatique du carbone

Le brassage a des conséquences profondes sur les microorganismes aquatiques, qui sont les moteurs des cycles biogéochimiques. En effet, ils représentent la base des réseaux trophiques (Butler *et al.* 2019; Rissanen *et al.* 2019) en participant à la production primaire, ainsi qu'au recyclage et à la transformation d'éléments essentiels (carbone, azote et autres nutriments). Par exemple, ils ont un grand rôle à jouer dans la décomposition pour recycler les nutriments de la matière organique issue des restes de plantes ou d'animaux et les rendre à

nouveau disponibles dans les réseaux trophiques (Capo *et al.* 2019). Également, la forme gazeuse de l'azote, le N_2 , n'est pas biodisponible par la majorité des organismes vivants, mais l'azote est un élément essentiel à la vie, et particulièrement à la photosynthèse : certains microorganismes ont la capacité de le fixer en ammoniac qui est assimilable, soutenant ainsi la production primaire. Ils sont aussi importants dans le cycle du carbone en milieu lacustre, particulièrement dans le cycle du CH_4 , où deux groupes de procaryotes se distinguent particulièrement et seront traités dans les prochaines sections.

1.1.4 Les méthanogènes

Le CH_4 est principalement produit par la méthanogénèse, une réaction effectuée par certains procaryotes en absence d'oxygène et responsable de 10 à 50% de la minéralisation du carbone en milieu lacustre (Borrel *et al.* 2011). Les méthanogènes (« producteurs de méthane ») sont des archées qui utilisent la méthanogénèse comme forme de respiration anaérobie et se servent de l'acétate ou du H_2/CO_2 pour produire de l'énergie en produisant du CH_4 grâce à l'enzyme de la méthyl-coenzyme M réductase (MCR) (Kotsyurbenko *et al.* 2004; Steinberg et Regan 2009; Albakistani *et al.* 2022). Cette réaction dépend de la température et de la disponibilité de la matière organique, mais surtout de l'absence de l'oxygène, ce qui la confine aux habitats anoxiques comme les sédiments lacustres (Samad et Bertilsson 2017) ou l'hypolimnion des lacs stratifiés (Youngblut *et al.* 2014). Le CH_4 produit par la méthanogénèse peut ensuite être relâché des sédiments vers la colonne d'eau soit par ébullition, par diffusion ou par transport en utilisant les plantes comme intermédiaire (Desrosiers *et al.* 2022). L'ébullition consiste en la migration rapide du CH_4 des sédiments à l'atmosphère sous forme de bulles en raison de son accumulation dans les sédiments, tandis que la diffusion comprend le CH_4 dissous dans l'eau. Cette forme dissoute est distribuée dans la colonne d'eau et peut être utilisée par un autre groupe de procaryotes, les méthanotrophes (Bastviken *et al.* 2004).

1.1.5 Les méthanotrophes

Les méthanotrophes (« qui se nourrit de méthane ») sont des bactéries qui oxydent le CH₄ et rejettent du CO₂ en conditions aérobies (Albakistani *et al.* 2022). La méthanotrophie est réalisée via une enzyme monooxygénase, majoritairement particulaire (pMMO) encodée par le gène *pmoA*, mais qui peut aussi parfois être soluble (sMMO) où elle est encodée par le gène *mmoX* (Morris *et al.* 2002; Knief 2015). La pMMO est l'enzyme utilisée par la plupart des groupes méthanotrophes à l'exception de quelques membres de la famille *Beijerinckiaceae*, tels les *Methyloferula* et *Methylocella* qui utilisent plutôt la sMMO (Dedysh *et al.* 2000; Dedysh *et al.* 2015; Knief 2015). Les méthanotrophes appartiennent à deux phyla bactériens : les Pseudomonadota et les Verrucomicrobia. Dans ce premier, les communautés méthanotrophes sont retrouvées dans l'ordre des *Gammaproteobacteria*, que l'on appelle les méthanotrophes de type I, et dans les *Alphaproteobacteria*, le type II (Knief 2015). Le seul ordre de méthanotrophes dans le phylum des Verrucomicrobia est celui des *Methylacidiphilales* (Dunfield *et al.* 2007; Pol *et al.* 2007; Knief 2015).

Les méthanotrophes sont omniprésents en milieu lacustre (Samad et Bertilsson 2017) et ont besoin de CH₄ comme source d'énergie, qu'ils peuvent acquérir lorsque le CH₄ produit dans les sédiments anoxiques diffuse à travers la colonne d'eau oxygénée (Samad et Bertilsson 2017). En raison de leurs besoins en oxygène et en CH₄, qui ont une distribution typiquement opposée dans les lacs en été (soit l'oxygène disponible dans l'épilimnion et le CH₄ dans l'hypolimnion), les méthanotrophes se trouvent principalement aux interfaces oxyques/anoxiques de la colonne d'eau. Ces interfaces incluent la thermocline en cas de stratification (où oxygène et CH₄ sont présents, quoiqu'à de faibles concentrations) ou à la surface des sédiments (là où le CH₄ est le plus disponible) si l'entièreté de la colonne d'eau est oxygénée. Bien que leur abondance est habituellement faible par rapport aux autres procaryotes lacustres, ils ont un grand rôle dans le cycle du carbone puisque leur taille cellulaire est plus

grande et que leur activité spécifique (consommation de carbone par unité de biomasse) est plus élevée que la plupart des autres bactéries hétérotrophes (Reis *et al.* 2022). Une étude par Reis *et al.* (2022) a trouvé que les lacs tempérés riches en carbone organique dissous et ayant un hypolimnion plus volumineux peuvent soutenir une consommation du carbone plus élevée par la méthanotrophie que par l'hétérotrophie, suggérant que cette voie métabolique serait plus importante que précédemment attendue malgré la faible représentation des méthanotrophes (<1% de la communauté bactérienne totale) (Reis *et al.* 2022). Ceci souligne l'importance potentiellement sous-estimée des organismes méthanotrophes dans le cycle biogéochimique du carbone des lacs boréaux. De plus, puisque les méthanotrophes se trouvent dans la colonne d'eau, il y a une opportunité pour le CH₄ produit par les méthanogènes dans les sédiments anoxiques d'être oxydé par la méthanotrophie avant sa diffusion dans l'atmosphère (Jansen *et al.* 2021). Par conséquent, les méthanotrophes sont considérés comme des biofiltres puisqu'ils peuvent réduire les émissions nettes de CH₄ des lacs (Knief 2015; Samad et Bertilsson 2017). Plusieurs études estiment que le pourcentage de CH₄ oxydé au sein de différents lacs se situerait entre 45% et 93% (Fallon *et al.* 1980; Frenzel *et al.* 1990; Utsumi *et al.* 1998; Bastviken *et al.* 2002; Kankaala *et al.* 2006).

1.1.6 La portée de la limnologie hivernale

Le cycle du CH₄ dans les lacs est bien connu lors de la saison estivale, qui est étudiée plus fréquemment et depuis plus longtemps que la saison hivernale. En effet, bien que la lumière soit apte à pénétrer les lacs malgré le couvert de glace, en zone boréale, l'accumulation de la neige sur la glace au fil du temps réduit cette pénétration, ce qui limite la production primaire (Cavaliere *et al.* 2021; Jansen *et al.* 2021) (Figure 2). Une autre limitation de l'oxygène est que le couvert de glace empêche sa diffusion de l'atmosphère à la colonne d'eau, ce qui peut conduire à des conditions hypoxiques sous la glace en fin d'hiver (Cavaliere *et al.* 2021; Jansen *et al.* 2021). Ainsi, en plus de présenter divers obstacles à l'échantillonnage (accès

au site, gel de l'équipement, perforage de la glace, sécurité, etc.) (Salonen *et al.* 2009; Block *et al.* 2019), les eaux froides, la limitation de la lumière et l'hypoxie sous le couvert de glace ont longtemps mené à croire que les lacs sont en état de dormance sous la glace (Tran *et al.* 2018) et donc que la recherche n'y est pas justifiée (Salonen *et al.* 2009). Toutefois, si lors de la saison sous couvert de glace la biomasse des organismes aquatiques est souvent réduite en raison des limitations de température, de l'apport de nutriments et de la qualité des substrats organiques, ces organismes sont toujours actifs contrairement aux idées préconçues (Schütte *et al.* 2016; Tran *et al.* 2018). D'ailleurs, plusieurs adaptations ou tolérances permettent la présence et l'activité des microorganismes sous la glace (Imbeau *et al.* 2021) et la présence d'activité microbienne est fortement suggérée par l'accumulation de gaz sous la glace (Jansen *et al.* 2021). Bien que l'hiver soit une saison sous-étudiée en limnologie, il revêt donc une importance cruciale pour l'équilibre de ces écosystèmes (Denfeld *et al.* 2018b; Block *et al.* 2019) et représente typiquement la moitié de l'année en zone boréale. Également, il est de plus en plus évident que la durée de la saison hivernale, le moment de la formation et de la fonte de la glace, ainsi que les processus sous la glace ont un impact sur la productivité estivale (Bertilsson *et al.* 2013; Block *et al.* 2019; Hébert *et al.* 2021).

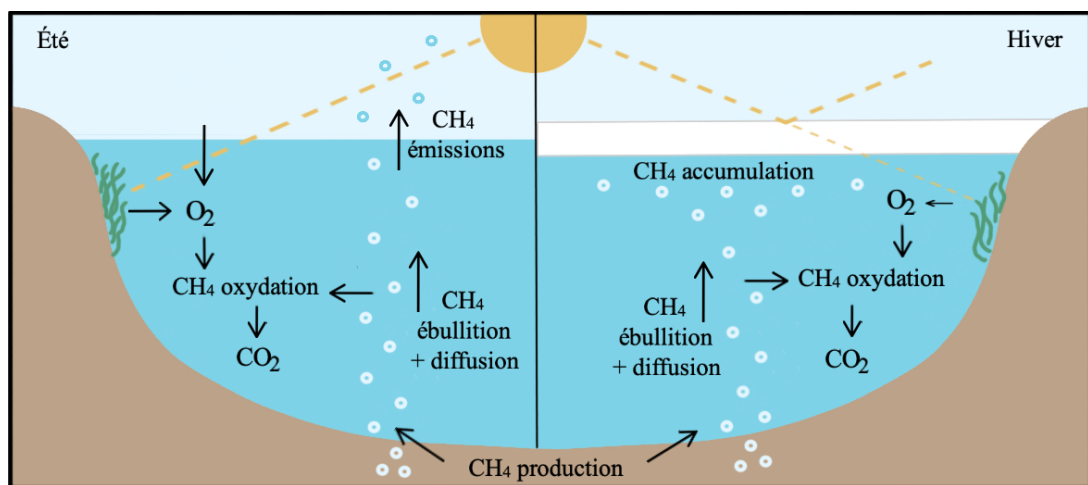


Figure 2 Sources de méthane et d'oxygène dans un lac boréal en été et en hiver, adapté de Li et Xue (2021) sous licence CC BY.

Il y a un intérêt croissant pour l'écologie microbienne sous la glace, et des études récentes ont démontré que les méthanotrophes seraient plus abondants en hiver qu'en été (Samad et Bertilsson 2017; Albakistani *et al.* 2022), suggérant un métabolisme hivernal potentiel du CH₄. En effet, la barrière formée par le couvert de glace limite l'entrée d'oxygène nécessaire au métabolisme des méthanotrophes, mais empêche également la diffusion du CH₄ et du CO₂ vers l'atmosphère : ces gaz s'accumulent alors sous la glace jusqu'au printemps (Miettinen *et al.* 2015; Denfeld *et al.* 2018a; Imrit et Sharma 2021) (Figure 2). Il y a donc une opportunité pour les méthanotrophes d'oxyder plus de CH₄ en hiver et de contribuer à la diminution des émissions lors de la fonte de la glace qui sont en plus amplifiées par le brassage printanier qui mélange le CH₄ jusqu'à l'épilimnion (Jansen *et al.* 2021) et représenteraient jusqu'à 55% des émissions annuelles d'un lac sur quelques jours seulement (Bizic-Ionescu *et al.* 2014). Cependant, cette occasion peut être compromise par l'épuisement de l'oxygène du lac vers la fin de l'hiver, la méthanotrophie étant une réaction aérobie.

Avec le réchauffement climatique, la période de la saison avec un couvert de glace sur les lacs boréaux change (Sharma *et al.* 2021). Au cours du dernier siècle, la glace s'est formée en moyenne 11 jours plus tard et a fondu 9 jours plus tôt, ce qui réduit le couvert de glace des lacs de l'hémisphère Nord d'environ 19 jours sur un an (Imrit et Sharma 2021). Ceci aura forcément des conséquences sur les conditions d'anoxie soutenant la méthanogenèse, le temps disponible pour les méthanotrophes de consommer le CH₄ emprisonné sous la glace, et ultimement sur le rôle des lacs boréaux dans les émissions des GES. Cela démontre le besoin de séries temporelles hivernales afin de mesurer l'impact de l'apparition de la glace, de l'appauvrissement en oxygène et du dégel sur la méthanotrophie et les émissions de GES des lacs boréaux qui devraient changer avec la progression des changements climatiques.

1.1.7 Objectifs

Ce mémoire présente une étude temporelle du CH₄ et du CO₂ dans un lac boréal en hiver dans le but de comprendre le rôle des méthanotrophes au fil de la saison. Combiné au suivi saisonnier du CO₂ et CH₄ dissous dans l'eau, nous présentons la diversité et l'activité des communautés microbiennes (avec une attention particulière aux méthanotrophes) d'un lac boréal sur une période de 9 mois, soit pendant la stratification verticale précédant la formation du couvert de glace, au cours de l'hiver, ainsi que pendant et après la fonte du couvert de glace. Les sous-objectifs sont de 1) mesurer le rôle des paramètres physicochimiques de la colonne d'eau dans la structure des communautés microbiennes et des méthanotrophes des sédiments, de l'eau et de la glace; 2) mesurer l'activité d'un gène impliqué dans la méthanotrophie (*pmoA*) le long d'un gradient temporel (au fil des saisons) et d'un gradient spatial vertical (dans la colonne d'eau et les sédiments); et 3) corréler la présence et l'activité des méthanotrophes aux concentrations de CH₄ et CO₂ dissous dans la colonne d'eau et les sédiments.

1.2 Méthodologie

1.2.1 Site d'études

L'étude a été réalisée au Lac Simoncouche (48.23 °N, 71.25 °W, 347 m ASL) au Québec, Canada (Figure 3A). Le Lac Simoncouche est un lac boréal dimictique et mésotrophe de taille moyenne (0.83 km²) et peu profond (moyenne de 2.2 m, maximum (z_{max}) de 8 m) (Kivilä *et al.* 2023). Le couvert de glace sur le lac dure habituellement du mois de novembre au début du mois de mai (données non publiées). Le site d'études ainsi que les méthodes complètes sont détaillés dans le Chapitre 2.

1.2.2 Plan d'échantillonnage

L'échantillonnage a eu lieu au point le plus profond du lac (Figure 3B) de septembre 2022 à mai 2023. Le lac a été échantillonné environ tous les 30 jours, à l'exception de décalages forcés par la formation et la fonte de glace, qui limitaient l'accès sécuritaire à z_{max} . La température et la concentration en oxygène dissous (DO) de la colonne d'eau ont été mesurées afin d'avoir des données sur la stratification du lac, puis, lorsque présentes, l'épaisseur de la glace et de la neige sur le lac ont été mesurées.

Trois différents habitats ont été échantillonnés sur un transect vertical dans le lac : la surface des sédiments (10 cm), la colonne d'eau (7, 3 et 0 m de profondeur) et la glace (lorsque présente). Tous les échantillons ont été manipulés de manière aseptique à l'aide de gants et d'outils rincés à l'éthanol pour éviter les contaminations, puis ils ont été conservés dans l'obscurité à 4 °C jusqu'à leur traitement en laboratoire pour conserver leur intégrité. Des échantillons de CH₄ et de CO₂ dissous ont été prélevés dans l'eau et les sédiments à l'aide de seringues qui ont été secouées pour libérer les gaz dissous.

1.2.3 Traitements des échantillons

L'eau des différentes profondeurs a été analysée pour mesurer la concentration de nutriments tels que l'azote total (TN), le phosphore total (TP), le carbone organique dissous (DOC) et quelques fractions de la matière organique dissoute colorée (CDOM) comme l'absorbance UV spécifique à 254 nm et la pente spectrale à 285 nm (S_{285}) qui indiquent l'aromaticité et le poids moléculaire du DOM, puis le coefficient d'absorption à 440 nm (a_{440}) qui a été utilisé pour quantifier le CDOM. De l'eau de chaque profondeur de la colonne d'eau et des carottes de glace fondues a été filtrée pour concentrer les microorganismes sur des filtres qui ont été utilisés pour l'extraction des acides nucléiques microbiens (ADN et ARN).

1.2.4 Séquençage et analyses bio-informatiques

Le séquençage de l'ADN a été utilisé pour décrire la composition des communautés microbiennes des sédiments, de l'eau et de la glace en ciblant les régions V3-V4 du gène de l'ARNr 16S à l'aide des amorces F341 et R805 (Herlemann *et al.* 2011). Le gène 16S code pour une sous-unité du ribosome procaryote, une machinerie cellulaire essentielle qui traduit l'ARN en protéines. Ainsi, toutes les bactéries possèdent ce gène qui présente diverses régions variables permettant de retracer la phylogénie des microorganismes séquencés et de résoudre leur taxonomie, afin de réaliser des analyses de diversité écologique (incluant l'indice de Shannon et la dissimilarité Bray-Curtis). Les abondances relatives ont été illustrées et les genres méthanotrophes ont été identifiés grâce à Dedysch et Knief (2018).

1.2.5 Quantification de gènes par PCR quantitative

Une réaction de polymérisation en chaîne quantitative (qPCR) a été effectuée sur l'ARN extrait des sédiments et de l'eau et rétroconverti en ADNc. En ciblant l'ARN converti en ADNc, nous obtenons de l'information sur les gènes actifs des communautés au moment de l'échantillonnage. Contrairement à la PCR, une approche qualitative qui permet de détecter la présence d'un gène, la qPCR quantifie précisément les acides nucléiques d'intérêt initiaux dans un échantillon en suivant la progression de l'amplification des gènes. Nous avons ciblé le gène *pmoA* qui code pour la sous-unité β de l'enzyme monooxygénase particulaire (Hanson et Hanson 1996; Knief 2015) qui effectue la méthanotrophie à l'aide des amorces A189F et mb661R (Costello et Lidstrom 1999).

1.2.6 Analyses statistiques

Pour la plupart des analyses statistiques, les échantillons ont été groupés en saisons selon les données de saturation en oxygène dissous (DO) et de la température (Figure 2). Les différences entre la moyenne des groupes ont été testées à l'aide d'un test de Wilcoxon et d'un

test de Dunn post hoc, le tout avec un seuil alpha de 0,05 et une correction de Bonferroni pour les comparaisons multiples, qui est parmi les corrections les plus conservatrices. Deux analyses d'importance relative des variables (RVI) ont été effectuées sur le meilleur modèle linéaire pour déterminer le poids relatif de chaque variable (environnementale ou groupe de méthanotrophes) dans le nombre de copies d'ADNc provenant de la qPCR (proxy pour l'expression des gènes). Les méthodes statistiques détaillées sont présentées dans le chapitre suivant.

CHAPITRE 2: Methanotrophy throughout winter and shoulder seasons in a boreal lake

2.1 Introduction

The boreal region contains a high density of lakes making up for at least 10% of its territory (Rasilo *et al.* 2015). These lakes play a considerable role in the carbon cycle: they are typically hotspots for the storage, processing and production of greenhouse gases (GHG) such as carbon dioxide (CO₂) and methane (CH₄), which are then released to the atmosphere by diffusion (Cole *et al.* 2007; Williamson *et al.* 2009; Rasilo *et al.* 2015). CO₂ can either originate from allochthonous or autochthonous sources, meaning it can come from the watershed or be produced internally via cellular respiration (Cole *et al.* 2007) or by microbial mineralization of dissolved organic carbon (Denfeld *et al.* 2018a), as well as abiotic production mechanisms. CH₄ is mainly produced by methanogenesis, which accounts for 10% to 50% of carbon mineralization in lakes and is carried out by methanogenic microorganisms, mostly in anoxic conditions (Borrel *et al.* 2011). Many biogeochemical processes that cycle carbon in lakes are therefore performed by microbial communities (Rissanen *et al.* 2019), although models used to describe these processes are often too broad to recognize the contribution of microorganisms (Juottonen *et al.* 2020).

In lakes, CH₄ transformations are mainly driven by two groups of microorganisms. These include archeal methanogens that use methanogenesis as a form of anaerobic respiration, using acetate or H₂/CO₂, to produce energy and CH₄ (Kotsyurbenko *et al.* 2004; Steinberg et Regan 2009) via a methyl coenzyme M reductase (MCR) (Steinberg et Regan 2009; Albakistani *et al.* 2022). The most common orders of methanogens found in freshwater sediments are *Methanomicrobiales* and *Methanosarcinales*, the most common genera being hydrogenotrophic (Borrel *et al.* 2011). Methanogenesis depends on temperature and on availability of organic matter, but mostly on the absence of oxygen, restricting it to anoxic habitats such as lake sediments (Samad et Bertilsson 2017), and CH₄ produced through

methanogenesis can be released from sediments either by diffusion, ebullition or plant-mediated transport (Desrosiers *et al.* 2022). CH₄ may subsequently be metabolized in the sediments or the water column by methane-oxidizing bacteria (MOB) through methanotrophy, a reaction that oxidizes CH₄ to CO₂ under aerobic conditions (Albakistani *et al.* 2022). Methanotrophy is performed via a monooxygenase enzyme, which is mostly particulate (pMMO) but is sometimes soluble (sMMO), where it is encoded by the gene *mmoX* (Morris *et al.* 2002; Knief 2015). Molecular approaches have been used in recent years to detect methanotrophy, and the most frequently used marker is the *pmoA* gene, which encodes the particulate methane monooxygenase enzyme used by most methanotrophic taxa except some members of the *Beijerinckiaceae* family (Dedysh *et al.* 2000; Dedysh *et al.* 2015; Knief 2015). Methanotrophs are ubiquitous in lakes and require CH₄ as an energy source, which they can acquire as it diffuses from anoxic sediments through the oxygenated water column (Samad et Bertilsson 2017). Although their abundance is usually low, methanotrophs have a large role in carbon cycling due to their large cell sizes and a higher specific activity compared to other prokaryotes (Reis *et al.* 2022). A study by Reis *et al.* (2022) found that in DOC-rich temperate lakes with large hypolimnia, carbon consumption can be greater through methanotrophy than DOC-consuming heterotrophy. Furthermore, methanotrophs are aerobes and are found throughout oxygenated water columns, including in surface waters and oxic/anoxic interfaces, thus representing an opportunity for sediment-produced CH₄ to be oxidized before it is released into the atmosphere (Jansen *et al.* 2021). As a result, methanotrophs can be considered as a biofilter as they can reduce net CH₄ emissions from lakes (Knief 2015; Samad et Bertilsson 2017). Several studies estimated the percentage of CH₄ oxidized in lakes to vary between 45% and 93% (Fallon *et al.* 1980; Frenzel *et al.* 1990; Utsumi *et al.* 1998; Bastviken *et al.* 2002; Kankaala *et al.* 2006).

Around 86% of all lakes experience an ice-covered season every year (Korver *et al.* 2024), which can last for several months in boreal regions. During winter, the ice cover at the

surface of lakes limits gas exchanges with the atmosphere, preventing the release of GHG produced in the lake, but also the diffusion of oxygen into the water column (Leppäranta 2015). The thickening of lake ice and snow accumulation on it also reduces solar radiation, limiting primary production (Leppäranta 2015) which, combined with the diffusion barrier, can lead to oxygen-limiting conditions under ice, potentially allowing for anoxic conditions to develop in the hypolimnion during winter (Cavaliere *et al.* 2021; Jansen *et al.* 2021). Over the course of the ice-covered season, lake biota are further impacted and microbial biomass is reduced due to limitations in temperature, nutrient inputs, and quality of organic substrates (Schütte *et al.* 2016; Tran *et al.* 2018).

While winter is an understudied season in limnology, it is of critical importance in the energy, nutrient and gas (including GHG) balance of these systems (Denfeld *et al.* 2018b; Block *et al.* 2019), and there is growing evidence that the onset and duration of the ice-covered season as well as under-ice processes have impacts on summer productivity (Bertilsson *et al.* 2013; Hampton *et al.* 2017; Hébert *et al.* 2021). There is therefore a growing interest in microbial ecology under ice, and recent studies have found that methanotrophs are more abundant in winter than in summer (Samad et Bertilsson 2017; Albakistani *et al.* 2022), and that their abundance increases with depth (Samad et Bertilsson 2017). However, as climate warming progresses, the timing and duration of the ice-covered season on boreal lakes is changing (Sharma *et al.* 2021). Over the last century, ice has formed on average 11 days later and melted 9 days earlier, which reduces the ice cover of lakes in the North Hemisphere by approximately 19 days over a year (Imrit et Sharma 2021). This underscores the need for winter time series, to measure how ice onset, oxygen-depleted conditions in winter and ice-off control microbial production and emissions of GHGs from boreal lakes.

Here, we present a temporal study of microbial drivers of GHG cycling in a boreal lake. Combined with seasonal tracking of dissolved CO₂ and CH₄, we present a 9-month survey of the diversity and activity of microbial communities, particularly the vertical stratification of

methanotrophs prior to ice-on, during ice formation, over winter and during ice-off. More specifically, we aim to 1) describe how physicochemical conditions of the water column drive the diversity of the methanotrophs; 2) measure the activity of the gene involved in methanotrophy (*pmoA*) in the water column, the sediments and the lake ice; 3) link the presence, taxonomy and activity of methanotrophs with the concentrations of dissolved CH₄ and CO₂ in the lake. We thus aim to better assess the contribution of methanotrophs in decreasing CH₄ emissions from boreal lakes and estimate how the emissions change as winters shorten and ice cover decreases. We expected CH₄ production would increase during the ice covered season, but that methanotrophs (measured via sequencing) and their methanotrophic activity (measured by qPCR) would counter its accumulation under ice.

2.2 Materials and methods

2.2.1 Study site

The study was conducted in Lake Simoncouche (48.23 °N, 71.25 °W; 347 m ASL) Quebec, Canada (Figure 3A). Lake Simoncouche is a dimictic and mesotrophic boreal lake of medium size (0.83 km²) and shallow depth (on average 2.2 m, maximum [z_{\max}] 8 m) (Kivilä *et al.* 2023). Water residence time is approximately 50 days (Vachon et del Giorgio 2014) but varies seasonally. Lake Simoncouche is located within the balsam fir-white birch bioclimatic domain (Ministère des Ressources naturelles et des Forêts 2022) where annual temperature average 3.1 °C and total precipitation reach 928 mm (Environment and Climate Change Canada 2024). The lake's annual CO₂ net production is 82 g C m⁻² yr⁻¹ and mostly comes from hydrologic CO₂ inputs (Vachon *et al.* 2017). Overall, 68% of CO₂ is expected to exit the lake annually by emission into the atmosphere (Vachon *et al.* 2017). A previous study by Desrosiers *et al.* (2022) measured average summer surface water concentrations of CO₂ and CH₄ in the pelagic zone of 825 ppm and 312 ppm, respectively. At z_{\max} , those gases were only from the

diffusive carbon flux pathway, as ebullition was found to be negligible. The ice cover on Lake Simoncouche usually lasts from November to early May (average ice-on over the last 15 years: 19 November; average ice-off: 03 May, unpublished data).

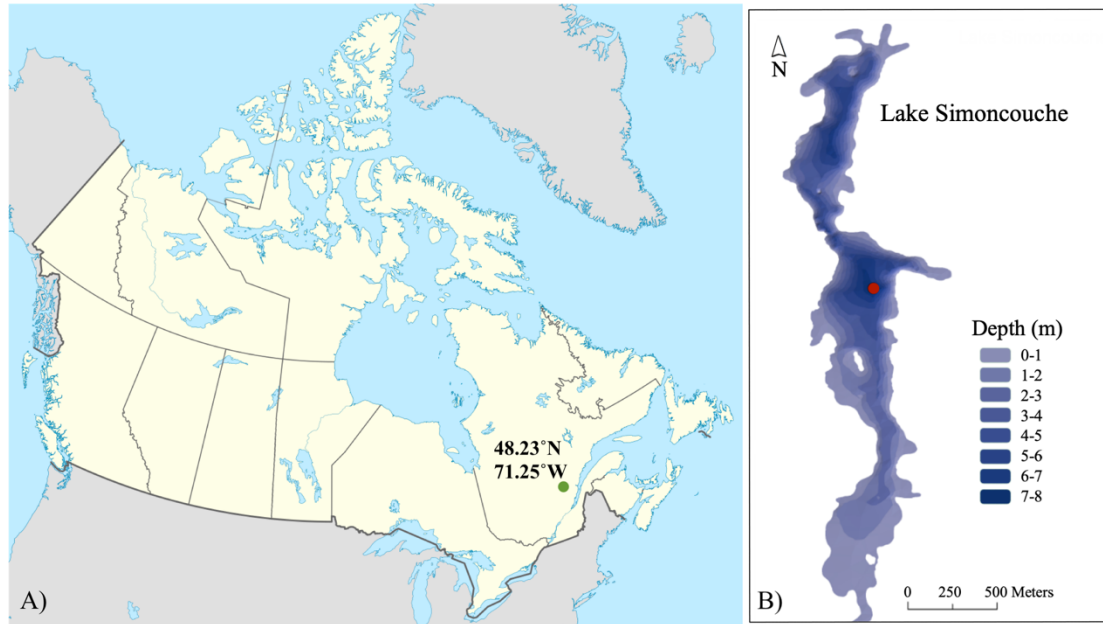


Figure 3 A) Location of Lake Simoncouche in Quebec, Canada (green point) and B) bathymetric map of Lake Simoncouche. The red point represents z_{max} . The map of Canada is from © Creative Commons under the license Attribution-Share Alike 4.0 International, the points and coordinates were added.

2.2.2 Sampling design

Sampling took place at the deepest point of the lake (Figure 3B) from fall 2022 to spring 2023. The lake was sampled roughly once a month between September 2022 and May 2023, with the first two and last two dates during open water: 22 September, 20 October, 1 December, 19 December, 19 January, 15 February, 15 March, 14 April, 27 April, and 24 May. Due to newly forming ice which limited our access to the deepest point of the lake on 1 December, sampling on this date occurred approximately 100 m to the north from z_{max} .

At each sampling event, water column temperature, conductivity, DO concentrations and chlorophyll *a* concentration were measured using a RBRconcerto CTD++ ® probe (Ruskin

RBR, Ottawa, Canada). During the ice-covered season, the water column was accessed through holes bored with a 20 cm diameter hand auger (Nils Master, South Burlington, USA). When present, ice and snow thickness were measured with a ruler.

Three different habitats were sampled in duplicate across a vertical transect in the lake: surface sediments (10 cm), the water column (0, 3 and 7 m) and ice (when present), for the analysis of nutrients, carbon and microbial communities. Sediments were collected using a Mini-Glew Sediment Corer (Queen's University, Kingston, Canada). Duplicate samples of approximately 50 mL of surface sediments were collected into sterile 120 mL Whirl-Pak™ bags (Whirl-Pak, Pleasant Prairie, USA) with ethanol-washed tools. Water samples were collected using a 2 L Limnos Water Sampler (Limnos.pl, Komorów, Poland) or a 4 L Kemmerer Water Sampler (Wildco, Saginaw, USA) and stored in 4 L Cubitainers™ (Fisher Scientific, Ottawa, Canada) that had been previously cleaned with 2% Contrad™ 70 liquid detergent (DeconLabs, King of Prussia, USA), 3.7% hydrochloric acid (Sigma-Aldrich, Saint-Louis, USA) and Milli-Q water, and rinsed three times with site water. Ice cores were collected with a Mark II corer (Kovacs Enterprise, Roseburg, USA) and stored in sterile 5441 mL Whirl-Pak™ bags. All samples were handled aseptically using ethanol-washed gloves and were stored in the dark at 4 °C until processing in the laboratory.

At each sampling event, samples for dissolved CH₄ and CO₂, were collected in triplicate using 60 mL (fall) or 140 mL (winter and spring) Monoject™ piston syringes (Cardinal Health, Dorval, Canada). After filling the syringes with either sediment or water, 30 mL were emptied and replaced with atmospheric air. Syringes were shaken for a few minutes and 20 mL of equilibrated headspace air was pushed into nitrogen-flushed and vacuumed 12 mL Exetainer® (Labco, Lampeter, UK) vials for gas analyses. Under ice cover, surface water samples were collected immediately after drilling the bore hole.

2.2.3 Sampling processing

Water subsamples were analyzed for nutrients and carbon at every time point. Total nitrogen (TN) and phosphorus (TP) were analyzed from 40 mL of unfiltered water at the GRIL Laboratory at Université de Montréal (Montreal, Canada). TN was analyzed on a Quikchem 8500 (Lachat Instruments, Milwaukee, USA, EPA method 353.2) and TP on an Astoria2 Analyzer (Astoria-Pacific, Clackamas, USA, EPA method 365.3).

Dissolved organic carbon (DOC) and colored dissolved organic matter (CDOM) were analyzed from water filtered with a Nalgene™ PVC manual vacuum pump and a reusable filter unit (Fisher Scientific) that had been washed with 10% hydrochloric acid, onto pre-burnt (4 h at 400 °C) 47 mm Whatman GF/F filters (Sigma-Aldrich). The filtrate was transferred into 40 mL amber vials (washed with 10% hydrochloric acid for 24 h, burnt at 400 °C for 6 h), and DOC was measured with a M5310C Total Organic Carbon Analyzer (Sievers Instruments, Oakville, Canada). To characterize CDOM the samples were scanned using Cary 100 Bio UV-Vis spectrophotometer (Agilent, Santa Clara, USA) from 850 nm to 220 nm with a 1 nm interval in a 1 cm cuvette. Spectral indices such as specific UV absorbance (SUVA; Weishaar *et al.* (2003)), spectral slope at 285 nm (S_{285} ; Helms *et al.* (2008)) indicate the aromaticity and molecular weight of DOM, while absorption coefficient at 440 nm (a_{440}) was used as a proxy of CDOM concentration.

Dissolved iron ions were analyzed with 40 mL of water and 200 µL of nitric acid as a preservative, transferred into Falcon® tubes previously washed with 10% hydrochloric acid. The samples were sent to the Institut national de la recherche scientifique (Quebec, Canada) and analyzed on an ICP-AES 5110 Dual View system (Agilent) using US EPA Method #200.7. Since high iron concentrations often lead to an overestimation of CDOM (Xiao *et al.* 2013), the spectral data of 22 September at 7 m were corrected using the following equation in Poulin *et al.* (2014):

$$a_{corrected} = a_{measured} - (0.0653 \times [Fe]).$$

Dissolved CO₂ and CH₄ concentrations were measured with a methaniser-equipped flame ionization detector. Two replicates of dissolved CO₂ and CH₄ concentrations from September-February samples were analyzed by Agriculture and Agri-Food Canada (Quebec, Canada) based on the method of Rochette et Bertrand (2008). The third replicate of every sample (September-May) was analyzed at the University of Lethbridge (Lethbridge, Canada) using a Trace 1310 chromatograph (Fisher Scientific) (Chan *et al.* 2024).

Remaining water column samples as well as melted ice cores (melted in the dark over three days at 4 °C) were filtered using a FH100M peristaltic pump (Fisher Scientific) and L/S Masterflex® tubing (Masterflex, Gelsenkirchen, Germany) onto 0.22 µm Sterivex™ filters (Millipore, Burlington, USA). The tubing was previously washed by cycling 2% Contrad™ 70 liquid detergent, then Milli-Q water for an hour each through the system. The volume filtered per sample was on average 1347 ± 433 mL, and filtrations were stopped when the flow rate decreased due to clogging. Filters were purged of liquid then were filled with 2 mL of RNeasy™ stabilization solution (Invitrogen, Carlsbad, USA) and stored at -80 °C until nucleic acid extraction.

2.2.4 Nucleic acid extraction

Nucleic acids (DNA and RNA) from sediments were extracted directly with the DNeasy® PowerSoil® Pro kit for DNA and RNeasy® PowerSoil® Total RNA Kit for RNA (QIAGEN, Hilden, Germany), following the manufacturer's instructions. For water and ice, nucleic acids were extracted from Sterivex™ filters with the AllPrep® DNA/RNA Mini Kit (QIAGEN) following the method of Cruaud *et al.* (2017). Quality of nucleic acids was measured using a Nanodrop™ 2000 spectrophotometer (Fisher Scientific), and DNA and RNA were quantified with a Qubit™ 4 fluorometer (Invitrogen) using the Qubit™ dsDNA HS and RNA HS Assay Kit (Fisher Scientific), yielding on average 8.82 ± 8.32 ng/µL DNA and 18.04 ± 36.32 ng/µL RNA (Table S1).

2.2.5 Sequencing and read processing

DNA sequencing was used to describe microbial communities from sediments, water, and ice over the sampling period. Sequencing libraries were prepared with 10 µL of DNA from all samples targeting the V3-V4 regions of the 16S rRNA gene using primers F341 (CCTACGGGNGGCWGCAG) and R805 (GACTACHVGGGTATCTAATCC) (Herlemann *et al.* 2011). Paired-end (2x300 bp) sequencing was performed on an Illumina MiSeq at the Institut de biologie intégrative et des systèmes (IBIS, Université Laval, Quebec, Canada), yielding 3 301 752 reads (average of 35 125 reads per sample) (Table S1).

Sequencing reads were processed in R software version 4.3.1 (R Core Team 2021) using the DADA2 library v.1.28.0 (Callahan *et al.* 2016) to filter and assemble paired DNA sequences. The quality filtering and trimming parameters were as follows: the truncation length was 280 bp in forward, 215 bp in reverse; maxEE was set at 2 in both directions, trimLeft was of 17 bp in forward and 21 bp in reverse. Reads were then filtered for chimeras, and remaining sequences were clustered into amplicon sequence variants (ASVs) to which taxonomy was assigned with the SILVA SSU database v.138 and SILVA Species Assignment v.138.1 (Quast *et al.* 2013; Yilmaz *et al.* 2014). The taxonomy table was later corrected at the order and family levels of methanotrophs and for every phylum according to the List of Prokaryotic names with Standing in Nomenclature (LPSN). Full sequence processing statistics are reported in Table S1. ASVs were used to build an abundance table: a raw table was used for alpha diversity analyses and a transformed table for beta diversity analyses. The latter was created by Hellinger transformation with the decostand function and a log transformation using the log10 function, both from the vegan library v.2.6.4 (Oksanen *et al.* 2017). Both abundance tables were joined separately to a taxonomy table and the sample data to create phyloseq-class objects with the phyloseq library v.1.44.0 (McMurdie et Holmes 2013) for community analyses. Chloroplast-assigned sequences and low abundance taxa (<0.05%) were removed from final datasets, and abundance tables were transformed into relative abundance for visualization.

2.2.6 Quantitative PCR gene quantification

Gene expression for the pMMO enzyme involved in methanotrophy was measured using quantitative polymerase chain reaction (qPCR) of the *pmoA* gene on RNA extracted from sediments and water. RNA was reverse transcribed to cDNA using the iScript™ Reverse Transcription Supermix (Bio-Rad, Mississauga, Canada), with 4 µL of iScript and 16 µL of RNA normalized with UltraPure™ nuclease-free water (Invitrogen) for each reaction. This produced on average 1.063 ± 0.48 ng/µL cDNA per sample (Table S1). From cDNA, we targeted the *pmoA* gene which encodes the β subunit of the pMMO enzyme (Hanson et Hanson 1996; Knief 2015), with primers A189F and mb661R (Costello et Lidstrom 1999). Primer pair specificity was confirmed with PCR (Method S1, Figure S1). The qPCR reactions were performed in 20 µL volumes as follows: 10 µL of SsoAdvanced Universal SYBR™ Green Supermix (Bio-Rad), 0.1 µL of each primer (x2), 2 µL of cDNA template and 7.8 µL of UltraPure™ nuclease-free water. No template controls (NTC) were included, and a standard curve was performed using gBlocks in seven-time dilutions 1:10, beginning at 9 860 000 copies/mL. The gBlocks were ordered at Integrated DNA Technologies (IDT, San Diego, USA) and were designed using the *pmoA* gene of uncultured *Methylococcaceae bacterium* clone LD (length = 510 bp, accession number EU135968.1) as a methanotroph representative. The qPCR was performed in three technical replicates on four different plates on a CFX96 Touch Real-Time PCR Detection System (Bio-Rad) as follows: initial denaturation for 2 min at 95 °C, 39 cycles consisting of 10 s denaturation at 95 °C and 30 s annealing at 62 °C, followed by denaturation at 95 °C for 10 s and a melting curve from 65 °C to 95 °C (0.5 °C/cycle). The lid temperature was 105 °C. Selected qPCR products were migrated on a 1.5% agarose gel containing SYBR™ safe DNA Gel Stain (Invitrogen) at 100 V with a 100 bp DNA ladder (Invitrogen™) and visualized using a DigiDoc-It™ (UVP, Jena, Germany), to determine the presence of qPCR products by size (500 bp for *pmoA*) (Figure S2).

Samples with a quantification cycle (Cq) value greater than the lowest no template control (NTCs, Cq = 33.4) or 3 cycles lower were considered no different than the NTCs or absent and were removed from the analysis (Figure S3). Starting quantities (SQ) were used to get the copy number of *pmoA* transcripts in every sample. Standard curves were performed for each plate or averaged between plates when necessary. Final SQ values were calculated as follows:

$$\text{Copy nb /mL water} = \frac{\left(\left(\text{SQ (copies)} \times \left(\frac{1}{\text{qty cDNA}} \right) \right) \times \text{extraction output } (\mu\text{L RNA}) \right)}{\left(\text{qPCR input } (\mu\text{L cDNA}) \times \left(\frac{\text{input cDNA reaction } (\mu\text{L RNA})}{\text{total cDNA reaction } (\mu\text{L cDNA})} \right) \right)} \times \text{qty filt. water or sediment input (mL)}$$

where SQ is the starting quantity estimate from qPCR analyses (copy nb), 1/cDNA is the ratio to equilibrate the total DNA input in the qPCR reaction, the extraction output is of 35 μL of RNA in water or ice samples and of 100 μL in sediment samples, the qPCR input was 2 μL of cDNA. The input to the cDNA reaction was either 1, 2, 5 or 16 μL of RNA, for a total of 20 μL of cDNA. The total was divided by either the quantity of water filtered for ice and water samples (Table S1), or by the sediment volume input of 3 mL.

2.2.7 Statistical analyses

For most statistical analyses, samples were binned into “seasons”, separated as follows based on DO saturation and temperature data (Figure 2): fall (22 September, 20 October, 01 December), early winter (19 December, 19 January), late winter (15 February, 15 March, 14 April) and spring (27 April, 24 May). Differences between seasons were tested with a Wilcoxon test with the function `pairwise.wilcox.test (stats)` and a post hoc Dunn’s test with the function `dunn_test` from the library `rstatix v.0.7.2` (Kassambara 2023), with an alpha threshold of 0.05 and a Bonferroni correction for multiple comparisons. Two relative variable importance (RVI) analyses were performed to rank every possible linear model by Akaike information

criterion (AIC) using different modeling functions in the library MuMIn v.1.47.5 (Bartoń 2024). The models were calculated between cDNA copy number from qPCR (proxy for gene expression) and 1) continuous environmental variables or 2) abundance of the dominant methanotrophic genera (sequencing data). From the best models, the relative weight of each variable was calculated and plotted, and a negative relation was determined based on the correlation matrix.

The Shannon index was used to compare alpha diversity and community evenness across habitats (ice, water, sediment) and over time with the function `estimate_richness` (phyloseq). Bray-Curtis dissimilarity was used to ordinate a non-metric multidimensional scaling (NMDS) for community patterns with the function `ordinate` (phyloseq). A PERMANOVA was performed to measure the difference between habitats with the function `adonis2` followed by a `betadisper` analysis to measure the homogeneity of the group dispersion (both in `vegan`). A cluster analysis was performed with the function `kmeans` in the `stats` library v.4.3.1 (R Core Team 2021) in order to statistically test sample partitioning by habitat. Relative abundance plots were made using the `plot_bar` function (phyloseq). Methanotrophic genera were identified from Dedysh et Knief (2018). When stated, low abundance genera were grouped as “Others” to improve visualization. Data were manipulated with the `dplyr` library v.1.1.2 (Wickham *et al.* 2023), and plots were created with the `ggplot2` library v.3.5.1 (Wickham 2016).

2.2.8 Data availability

The sequencing data are available at NCBI Sequence Read Archive (SRA) under BioProject ID PRJNA1119568.

2.3 Results

Ice formed on Lake Simoncouche on November 20 and melted on April 28, lasting 5.3 months (Figure 4A). Maximum ice thickness (59 cm) was measured on March 15, while the snow thickness was stable (23.5 ± 0.5 cm) from January to March.

Seasonal variations of DO and temperature displayed typical mixing and winter stratification patterns for boreal lakes (Figure 4B), with the entire water column mixing in October (fall overturn). The inverse temperature stratification was established in early winter (mid-December) and persisted until mid-April, where some perturbations were noticeable. DO decreased over winter in the bottom of the lake, down to 10.11% in the hypolimnion in March. DO increased in mid-April, but only in the hypolimnion (51.53%). Spring mixing (spring overturn) of the water column began before the first April sampling date.

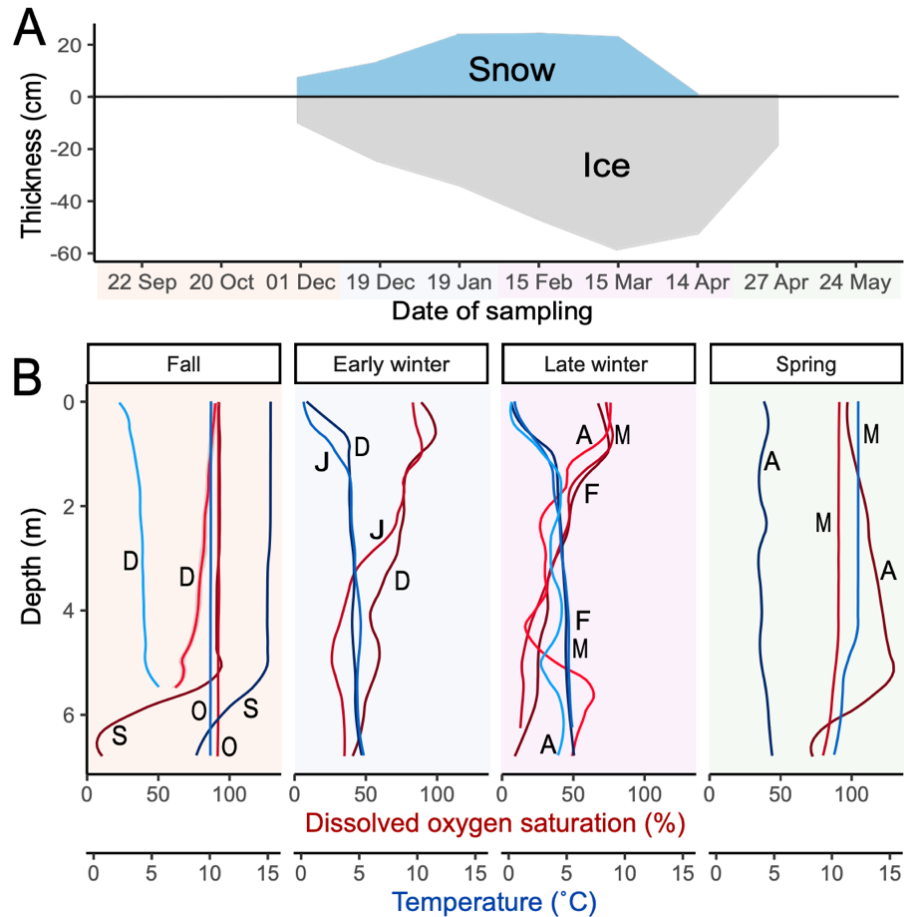


Figure 4 A) Ice and snow thickness over the sampling period. B) Dissolved oxygen (DO) (red) and temperature (blue) in the vertical column of the lake in fall (22 September, 20 October, 01 December), early winter (19 December, 19 January), late winter (15 February, 15 March, 14 April) and spring (27 April and 24 May). Within each season, months are identified by their first letter and colored from darker to lighter hues over time.

TN and carbon concentrations showed seasonal variations (Table 1). DOC concentrations were greater in the fall (6.71 ± 0.40 mg/L) and early winter (6.75 ± 0.59 mg/L) than in late winter (5.87 ± 0.59 mg/L) ($p < 0.05$). In contrast, TN was lower in the fall (0.39 ± 0.28 mg/L) than late winter (0.55 ± 0.39 mg/L) or spring (0.76 ± 0.70 mg/L) ($p < 0.05$). No significant differences were seen between seasons for TP, SUVA, S_{285} and a_{440} . As for vertical variations throughout the water column, some differences were observable across depths: S_{285} was higher at 3 m (0.0187 ± 0.000) than 7 m (0.0169 ± 0.002) while DOC was lower at 3 m

(6.38 ± 1.30 mg/L) than 7 m (6.71 ± 0.52 mg/L) ($p < 0.05$). Over the entire sampling season, the total average values for nutrients was 0.51 ± 0.35 mg/L for TN, 7.39 ± 4.38 μ g/L for TP and 6.45 ± 0.71 mg/L for DOC.

Table 1 Concentration of total nitrogen (TN), total phosphorus (TP), dissolved organic carbon (DOC) and spectral indices such as specific UV absorbance (SUVA), spectral slope at 285 nm (S₂₈₅) and absorbance coefficient at 440 (a₄₄₀) of CDOM. For variables with replicated samples, average values are provided together with standard deviation.

Sampling date	Depth (m)	TN (mg/L)	TP (μ g/L)	DOC (mg/L)	SUVA	S ₂₈₅	a ₄₄₀ (m ⁻¹)
22 September	0	0.28 ± 0.02	5.41 ± 0.20	6.84 ± 0.05	3.321	0.0172	2.705
	3	0.36 ± 0.02	5.68 ± 0.20	6.74 ± 0.05	2.956	0.0189	1.791
	7	1.15 ± 0.12	23.53	7.27 ± 1.07	0.412*	0.0120	0.542*
20 October	0	0.28 ± 0.02	7.2 ± 0.00	6.47 ± 0.05	2.961	0.0192	1.620
	3	0.26 ± 0.00	10.66 ± 4.11	6.82 ± 0.16	2.805	0.0190	1.856
	7	0.27 ± 0.01	7.62 ± 1.37	6.57 ± 0.03	2.964	0.0187	2.090
01 December	0	0.35 ± 0.02	5.54 ± 0.63	7.04 ± 0.17	2.780	0.0193	1.803
	3	0.30 ± 0.00	4.15 ± 0.74	6.36 ± 0.02	2.870	0.0193	1.661
	7	0.30 ± 0.00	3.59 ± 0.78	6.36 ± 0.02	2.841	0.0192	1.538
19 December	0	0.35 ± 0.01	7.24 ± 1.48	6.92 ± 0.26	2.977	0.0184	1.932
	3	0.32 ± 0.03	4.30 ± 0.59	6.22 ± 0.16	2.935	0.0191	1.564
	7	0.48 ± 0.04	5.32 ± 0.40	7.22 ± 0.40	3.031	0.0174	2.198
19 January	0	0.34 ± 0.02	5.16 ± 1.46	6.34	2.767	0.0183	1.811
	3	0.31 ± 0.02	4.37 ± 1.10	6.09	2.968	0.0183	1.629
	7	0.49 ± 0.05	5.12 ± 0.20	7.67	2.577	0.0179	1.687
15 February	0	0.36 ± 0.03	5.30 ± 0.00	5.43 ± 0.08	3.262	0.0178	2.224
	3	0.31 ± 0.01	4.65 ± 0.35	5.44 ± 0.01	3.125	0.0190	1.160
	7	0.51 ± 0.03	4.75 ± 0.21	6.55 ± 0.03	3.143	0.0173	1.766
15 March	0	0.35 ± 0.02	4.45 ± 0.07	5.37 ± 0.34	3.177	0.0186	1.929
	3	0.33 ± 0.03	4.20 ± 0.28	5.66 ± 0.13	3.108	0.0191	1.700
	7	0.57 ± 0.07	4.00 ± 0.28	6.40 ± 0.00	3.262	0.0168	2.432
14 April	0	1.18 ± 1.06	9.66 ± 0.87	5.45 ± 0.77	2.570	0.0175	1.168
	3	0.76 ± 0.22	12.29 ± 2.23	5.75 ± 0.04	3.006	0.0189	1.308
	7	0.59	7.24	6.85 ± 0.21	2.963	0.0165	1.776
27 April	0	0.49 ± 0.17	7.80 ± 4.10	6.19 ± 0.39	3.532	0.0149	2.728
	3	0.92 ± 0.12	4.95 ± 1.06	8.59 ± 3.98	3.081	0.0179	1.897
	7	1.89 ± 1.33	13.60 ± 7.64	6.60 ± 0.14	3.182	0.0156	2.410
24 May	0	0.37 ± 0.11	10.20 ± 1.84	6.36 ± 0.25	2.905	0.0176	1.948
	3	0.57 ± 0.26	7.05 ± 1.49	6.04 ± 0.02	3.056	0.0174	1.972
	7	0.35 ± 0.07	16.70	6.07 ± 0.11	3.012	0.0173	1.977

*Values corrected for high iron concentrations

Community pattern analyses over time revealed that microbial communities formed three statistically significant clusters (K-means clustering) (Figure 5A). Contrary to what we expected, habitat was not the only significant binning factor: it separated the sediments, but not the water and the ice. Cluster 1 was mainly composed of water and ice samples from January to end of April, cluster 2 included water samples from the ice-free season as well as 3 m and 7 m water samples and ice from 1 December, and cluster 3 was composed of all sediment samples as well as the September 7m water column sample. Samples from 19 December were split: ice and surface waters grouped into cluster 1, and the middle and bottom waters grouped into cluster 2. Clusters 1 and 2 are distinguished by differences in the relative abundance of Planctomycetota (10% vs 35%) and of Cyanobacteria (8% vs 0%) (Figure S4). Overall, there were some outliers which were explained by limnological processes like ice formation, ice melting or water column stratification: ice of 01 December was more similar to water samples, water from 0 m was similar to the ice from 27 April, and the hypolimnion of 22 September is halfway between water and sediment samples.

Microbial community composition of the water column exhibited changes progressively throughout seasons (Figure 5A). From September to April, the NMDS2 axis appeared to separate water samples chronologically. This trend was not observable for sediment and ice samples. Sample type and depth (ice, water at 0 m, 3 m or 7 m, sediments) explained a significant proportion of sample groupings (adonis, $R^2 = 0.3607$, $p < 0.05$, while within-habitat variance was not significant (betadisper, $p > 0.05$).

Across all habitats, taxonomic richness and evenness increased over time, and was lower in the fall than in late winter ($p < 0.05$) and spring ($p < 0.01$). There was no significant difference in taxonomic richness (including equitability) between habitats (Figure 5B).

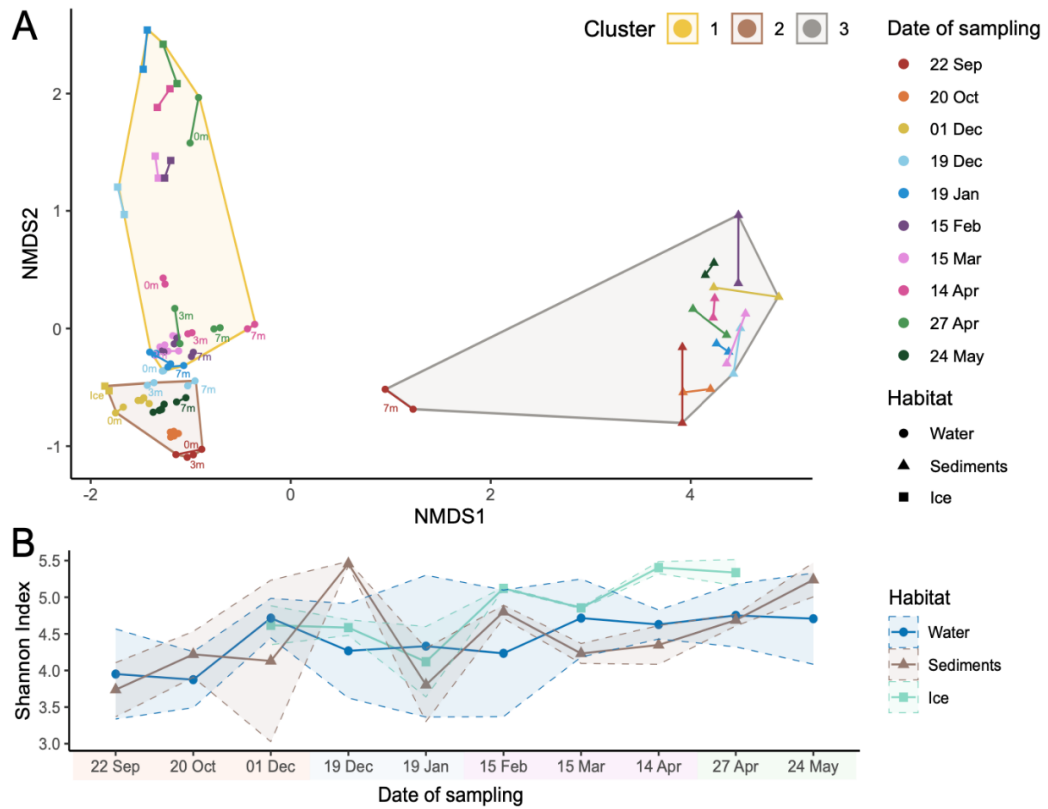


Figure 5 A) NMDS of Bray-Curtis dissimilarity of microbial communities of Lake Simoncouche represented by their habitat (water, sediments and ice) and sampling date, and with lines connecting biological replicates. B) Alpha diversity represented by the Shannon index for each habitat over time.

The relative abundance of some methanotrophic genera varied seasonally throughout the water column (Figure 6). *Methylobacter* peaked in late winter in surface water (0.121% of total community), then in late winter and spring at 3 m (0.03%) and 7 m (0.13%). *Candidatus Methyloacidiphilum* was dominant during the open water before the ice-in at 0 and 3 m, decreasing from 0.042% to 0.006% following fall mixing. Sediment methanotrophs did not show temporal variation, but were more diverse than water methanotrophs, and three genera were equally dominant: *Methylobacter*, *Methylocystis* and *Methyloparacoccus*. Ice samples followed the same temporal trends as surface waters, but at lower relative abundances.

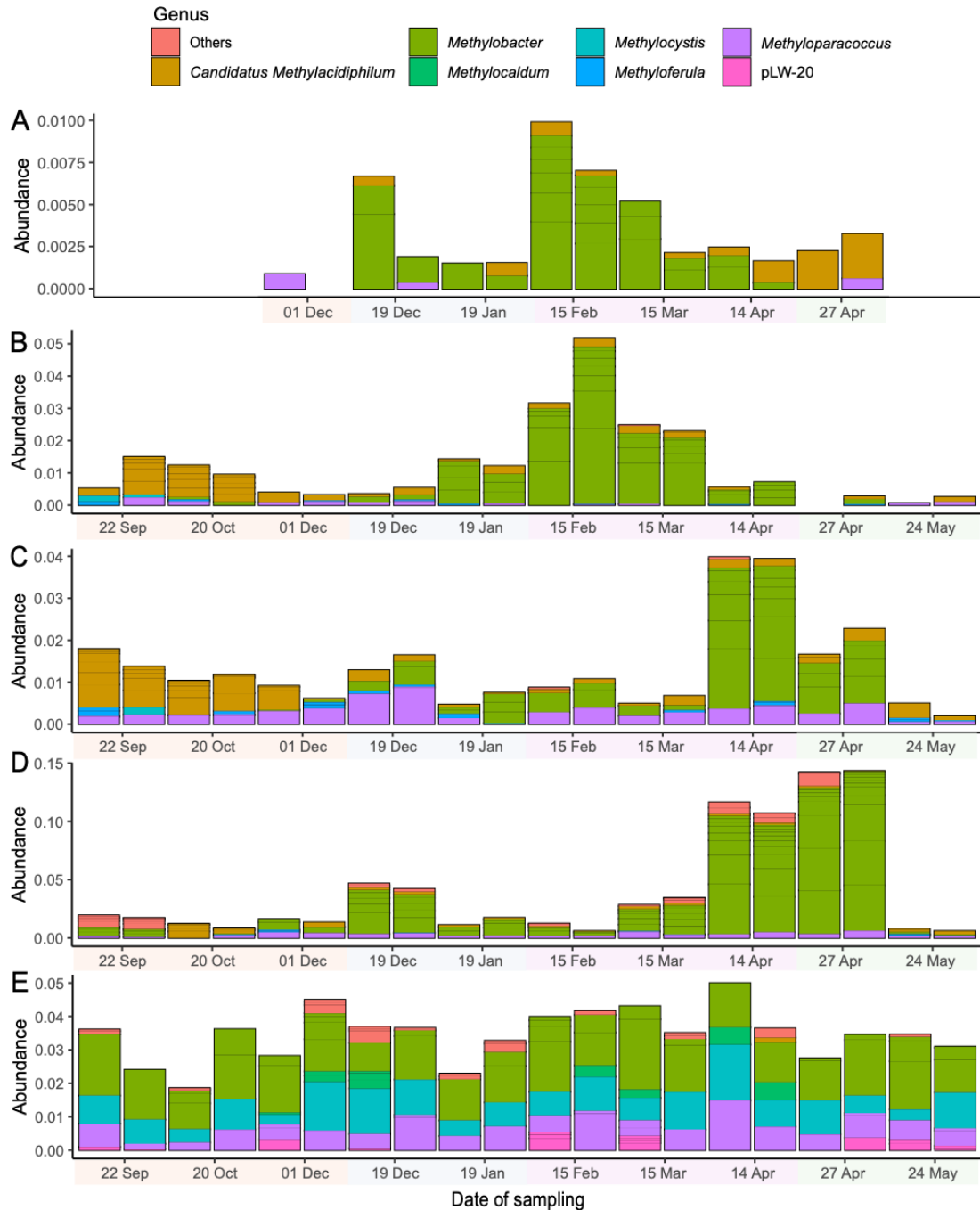


Figure 6 Relative abundance of methanotroph genera in duplicate samples based on sequencing of the 16S rRNA gene in A) the ice, B) 0 m water, C) 3 m water, D) 7 m water and E) sediments. Note different scales used across habitats. The dates on the x-axis are colored according to seasons. Low abundance genera were grouped in “Others”, and include *Methylomonas*, *Methylosphaera*, *Methyloterricola*, *Methylovulum*, *Methyloglobulus*, *Methylosinus*, *Methylosoma*, *Candidatus Methylospira* and *Methylomagnum*.

CH₄ concentration in the water column declined after fall mixing, first in the hypolimnion, then followed by surface waters (Figure 7A), decreasing from $0.64 \pm 0.2 \mu\text{M}$ in the fall to $0.21 \pm 0.3 \mu\text{M}$ in early winter ($p < 0.001$) and $0.24 \pm 0.4 \mu\text{M}$ in late winter ($p < 0.01$). It is important to note that the hypolimnion from September was not included in this average since the value considerably deviated from the dataset ($103.25 \pm 17.7 \mu\text{M}$). CO₂ accumulated over winter and peaked on 27 Apr before ice-out, it was higher in the late winter at $150.2 \pm 66 \mu\text{M}$ than in the fall at $96.96 \pm 141 \mu\text{M}$ ($p < 0.001$) or early winter at $61.82 \pm 35 \mu\text{M}$ ($p < 0.001$) (Figure 7C). In sediments, the same trend is noticeable for both gases: concentrations decreased during the ice-covered season from $805.28 \pm 293 \mu\text{M}$ to $314.24 \pm 188 \mu\text{M}$ ($p < 0.01$) for CH₄ and from 1283.62 ± 213 to $678.14 \pm 388 \mu\text{M}$ for CO₂ ($p < 0.01$) (Figure 7B and D).

Transcripts of the *pmoA* gene (coding for the enzyme enabling methanotrophy) were more abundant in the water column in April and May ($1.72 \times 10^4 \pm 1.93 \times 10^4$ copies/mL) than at any other moment ($3.20 \times 10^3 \pm 5.57 \times 10^3$ copies/mL) ($p < 0.01$) (Figure 7E). At these sampling events, they were also detected consistently at every depth of the water column, in contrast to the September-March period, where activity was detected in two depths in September (0 and 7 m) and March (0 and 3 m), one depth in both December (7 m) samplings and January (7 m), and none in October and February. Sediments had a greater transcript abundance in the fall ($1.86 \times 10^7 \pm 1.04 \times 10^7$) and in the spring ($1.46 \times 10^7 \pm 1.37 \times 10^7$) compared to early winter ($1.67 \times 10^6 \pm 1.41 \times 10^6$) ($p < 0.01$). Copy numbers were greater in sediments than in the water column at every sampling date ($7.16 \times 10^7 \pm 5.75 \times 10^7$ copies/mL compared to $\times 10^4$). Transcripts were detected in the ice in February and April. In total, 147 of 282 samples (including technical replicates) had a Cq value lower or equal to the NTC and were therefore removed from analyses (Figure S3). The disparity was greater between biological replicates than the technical ones.

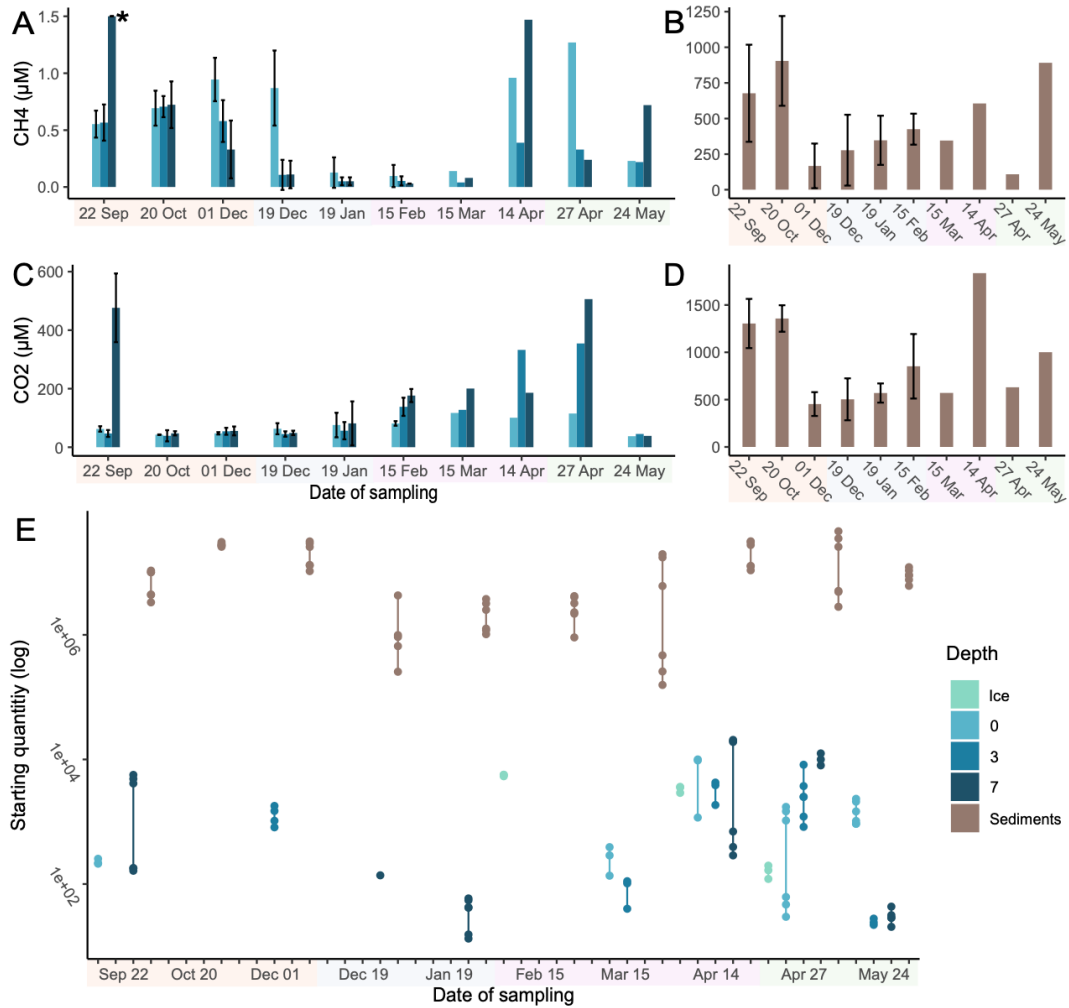


Figure 7 Dissolved CH₄ concentrations in A) the water column and B) the sediments; dissolved CO₂ concentrations in C) the water column and D) the sediments; and E) copy number of *pmoA* transcripts, every dot being a technical replicate (6 total per sample). *Original value at 103.25 ± 17.7 µM, cut for visibility.

The RVI analysis determined that the best model to explain the *pmoA* transcript copy number through environmental variables included TN and CH₄. Both showed a 100% weight in the analysis, while DO showed a negative relation with a 37% weight (Figure 8A). Only the most abundant methanotrophic genera were used in the models (excluding “Others”, Figure 6) and were separated by habitat. The best model in both selected habitats (water (Figure 8B), sediment (Figure 8C)) included *Methylobacter*, but in different scales : in the water, it had a

weight of 97% while it was only 35% and the relation was negative in the sediments. Ice habitat was not considered since there were only two time points with a *pmoA* copy number.

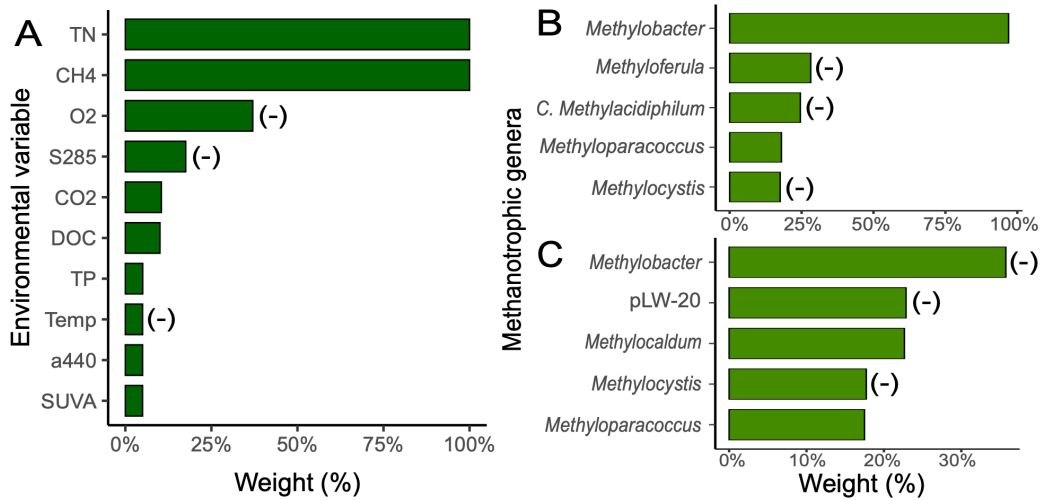


Figure 8 Relative importance weights (%) of A) environmental variables, and methanotrophic genera in B) the water column and C) sediments explaining copy numbers of the *pmoA* gene. The (-) indicates a negative relationship between the variables and the activity. C. stands for candidatus.

2.4 Discussion

2.4.1 Ice cover impacted Lake Simoncouche limnology

Physicochemical conditions varied over time, underscoring the impact of ice cover on a lake during winter. The first sampling (September 22) occurred before the water column had fully entered to fall overturn, explaining the hypoxia measured at 7 m (Figure 4B). Soon after, temperature and DO fully homogenized and lasted like this for weeks prior to the establishment of the inverse thermal stratification, which endured throughout winter. The main physicochemical variation defining the difference between early and late winter was dissolved oxygen concentrations in the hypolimnion. Oxygen was depleted (<2 mg/L) in late winter (February and March) at depths greater than 3.5 m, which was expected with continuous microbial respiration and with the absence of diffusion of oxygen from the atmosphere into the lake. This is consistent with observations of near bottom hypoxia under the ice cover, which

has been found to be common for shallow lakes (Cavaliere et Baulch 2021). While primary production under ice is possible (Kivilä *et al.* 2023), the presence of snow severely impedes the penetration of light into the water column. With snow thickness exceeding the threshold of 13.5 cm established by Pernica *et al.* (2017) from late December to late March on Lake Simoncouche, we expected primary production to be restricted, decreasing the production of oxygen in the lake without reducing its demand. Therefore, both ice as a diffusive barrier and snow as a light attenuator likely contributed to the depletion of oxygen in the water column from early to late winter.

Oxygen concentrations remained low throughout winter but did increase to 8.49 mg/L (130% saturation) in the hypolimnion in mid-April, although ice was still present on the lake. While this may be due to early primary production and to the melt of snow (Kivilä *et al.* 2023) allowing greater light penetration of the water column, this increase in oxygen was detected only at 5-6 m, below the photic zone. A more likely explanation is oxygen-rich water from a tributary river, which warms earlier than the lake and flows under the ice at a depth where density and temperature match with that of the river (unpublished data). Similar negatively buoyant plumes have been reported from other lakes during ice breakup (Forrest *et al.* 2011; Cortés *et al.* 2017). In April, when snow is melting in the watershed, water residency in the lake can be as low as 12 days (unpublished data), bringing more oxygen from the watershed into the lake. This underscores the importance of watershed-scale processes in under-ice oxygen availability in boreal lakes, especially in late winter. Following ice-out, the spring mixing took place, the temperature profile became homogenous and DO increased at every depth, as a dimictic lake model would usually show.

Nutrient data showed limited variations from September to May (Table 1) except for significant increases in TN and decreases in DOC. The rising concentrations of TN measured in Lake Simoncouche during winter support observations made on 30 lakes in the Northern hemisphere, 21 of which showed an increase of TN under ice (Hampton *et al.* 2017). This may

be due to winter nutrient mineralization in the sediments bringing new inputs of nitrogen, or to a limited uptake due to low temperature and limited oxygen, potentially impeding denitrification (Catalan 1992). The same study (Hampton *et al.* 2017), which included Lake Simoncouche, showed that lakes of similar size as Lake Simoncouche ($> 0.373 \text{ km}^2$) had lower winter DOC concentrations, a tendency the current study confirms. DOC comes from either autochthonous or allochthonous organic matter of plants, animals or phytoplankton in decomposition as well as soils and is an energy source (Kivilä *et al.* 2023) for heterotrophic organisms (Buchan *et al.* 2014). Its decrease in late winter can be linked to a lower supply of terrestrial carbon (Lepistö *et al.* 2014) and its continuous absorption by heterotrophic bacteria (Tulonen *et al.* 1994).

For geographical context, the concentration of TP, DOC, and the a_{440} values were lower than those measured in summer for 25 lakes in the area, including Simoncouche (Rasilo *et al.* 2015). This is likely caused by the reduced coupling between the watershed and lake during the winter months when the ground is frozen, leading to reduced inputs of both dissolved and particulate materials. Another mechanism is increased sedimentation of materials in the still water column under the ice, which was supported by the increasing DOC concentrations at greater depths.

Overall, nutrient levels in Lake Simoncouche (Table 1) were similar to those measured two years prior in the same lake (Kivilä *et al.* 2023), the exception being higher TP in the melting season (9.73 ± 2.53 in 2023 vs. 7.2 ± 2.78 in 2021 $\mu\text{g/L}$). However, the snow cover was thicker on the watershed and the ice cover melted two weeks later in the present study, which may explain higher TP concentrations from runoff water, resuspension from the sediments and a higher biological activity, underscoring the importance of the extent of runoff and timing of ice-off in nutrient availability.

2.4.2 Microbial communities varied under ice

Diversity and community evenness increased over time, as shown by Shannon diversity index values. This suggests that after fall mixing, taxonomic richness progressively stabilizes over the winter, as environmental conditions do (Butler *et al.* 2019). It then allows an increase in diversity over the new conditions in winter, as seen in Butler *et al.* (2019). Microbial communities from ice, water and sediments were expected to differ since these habitats present a diversity of physicochemical factors that impact the survival of microorganisms, separating them into distinct ecological niches. More specifically, in the sediments, there is a lack of oxygen and a greater presence of particles. As sediments present greater physical stability than the water column, they can support a greater microbial diversity (Li *et al.* 2023), and biomass and taxonomic richness are usually much greater than in water (Zinger *et al.* 2011). The water column is typically variable and possesses depth gradients of oxygen, light, temperature and nutrients, while lake ice has the lowest temperatures and is an oligotrophic environment with limited nutrients (Imbeau *et al.* 2021). Surprisingly, there was no difference in the taxonomic richness between the different habitats of samples. The similar diversity between water and sediments could be due to the recalcitrant nature of sediments for the nucleic acid extraction as the average DNA quantification did not differ between the habitats (19.6 ± 18.7 ng/ μ L in water vs. 14.4 ± 9.7 ng/ μ L in the sediments). Further, considering that the ice community started with the inclusion of microbes from the water in December, there is a time point where the communities were the same. Even with the addition of snow ice later in the season and likely associated microbes, ice and water never differentiated enough to be statistically distinguished.

The three clusters of microbial communities in Figure 5A were not formed solely by the habitat (ice, water, sediment), like the third cluster, which was dominantly composed of sediment samples. In the first two clusters, a temporal separation was observed, showing evidence of the impact of the ice cover on the water column and demonstrating the importance

of ice formation on aquatic communities not only directly under ice, but also at greater depths. The presence (or absence) of ice was the main driver for clusters 1 and 2, except for the entire water column from 1 December, and water from 3 and 7 m collected on 19 December. This suggests that there is a slight temporal lag before the presence and increasing thickness impact the water column (particularly at greater depths), and this progresses from the lake surface to deeper depths. In terms of composition, the major difference in cluster 2 compared to cluster 1 was the increase of Planctomycetota, a phylum commonly found in boreal and subarctic wetlands, freshwater habitats and soils, but whose ecological functions are not fully understood (Kulichevskaya *et al.* 2020). Only two families represented this phylum in our samples, *Gemmataceae* which is aerobic, chemoorganotrophic and characterized by large genome sizes (Kulichevskaya *et al.* 2020), and *Pirellulaceae* which is often detected on biofilms on macroalgae (Ivanova *et al.* 2018).

Methanotrophs identified from V3-V4 16S sequencing accounted for a limited proportion of whole microbial communities (0-15%), consistent with observations made by Mayr *et al.* (2019) in a holomictic lake in Switzerland (peak at 11-26%). However, other studies found them to range up to 58-60% in boreal lakes, mostly in summer (Rissanen *et al.* 2018; Martin *et al.* 2021; Albakistani *et al.* 2022). Methanotrophs are found in the phyla Pseudomonadota and Verrucomicrobia (Figure S4), and their presence in Pseudomonadota is classified in *Gammaproteobacteria* (type I) and *Alphaproteobacteria* (type II) (Knief 2015). All seasons combined, type I methanotrophs were dominant (genera *Methylobacter*, *Methylocaldum*, *Methyloparacoccus*, pLW-20 and some others, Figure 6) consistent with many other studies of freshwater lakes (Samad et Bertilsson 2017; Rissanen *et al.* 2018; Mayr *et al.* 2019; Martin *et al.* 2021; Albakistani *et al.* 2022).

In the water column, *Methylobacter* peaked in winter and spring (Figure 6), similar to observations reported by Albakistani *et al.* (2022). However, *Methylovulum* was less abundant, being present in only two samples at a relative abundance of 0.0006% to 0.0013%. Albakistani

et al. (2022) also found that *Methyloparacoccus* increased in the fall compared to spring, while our study detects them mostly at 3 m with a peak in mid-December, and in the sediments.

In the fall, there was a dominance of the *Candidatus Methyloacidiphilum* group in the water column at 0 and 3 m, before they disappeared after the fall mixing. This genus is the only representative of the phylum Verrucomicrobia in the methanotrophs we identified, and its order can be referred as V6 (Tran *et al.* 2018). In Tran *et al.* (2018), Lake Simoncouche was compared to two other boreal lakes, and it was found that, for these lakes, V6 were more abundant in the ice-free period compared to ice-covered, which agrees with the decrease we observed. In May, the relative abundance of methanotrophs drastically decreased throughout the water column. A lower relative abundance of methanotrophs in summer has been reported (Samad et Bertilsson 2017), as grazing on methanotrophs can increase due to higher abundance of organisms of higher trophic levels. Type I methanotrophs, which were dominant in our samples, possess larger cell sizes and may thus be more likely to be grazed (Jansen *et al.* 2021; Reis *et al.* 2022).

A large diversity of methanotrophs was also detected in sediments and did not change over time as observed by other studies (Pester *et al.* 2004; Tsutsumi *et al.* 2012). Others, however, have found temporal changes in methanotroph assemblages in sediments (Yang *et al.* 2020; Lyautey *et al.* 2021). Lyautey *et al.* (2021) found that depending on the site, the dominant genus in the sediments was either *Methylobacter* or *Methylococcus*. This last genus was also a dominant group in the five Swiss lakes studied by van Grinsven *et al.* (2022) and has previously been isolated from freshwater sediments (Bowman Jr. 2015), but was not detected in our study. In comparison, dominance in the sediments was shared by *Methylobacter* with *Methyloparacoccus* and *Methylocystis*. No significant seasonal variation was observed, either during mixing events, potentially oxygenating the surface of the sediments, or when the hypoxia extended from the bottom of the lake up to 4 m depth, limiting access to oxygen.

Methylocystis and pLW-20 genera were found more consistently in sediments, and only sporadically in the water column.

An important limitation to using DNA as an indicator with sequencing is that this tool cannot quantify absolute counts due to potential biases in DNA amplification prior to sequencing, nor can it guarantee the activity or viability of the cells: some can be dormant or dead (Reis *et al.* 2024). Indeed, some groups can form cysts (*Methylobacter*, *Methylocaldum*, *Methylocystis*) in unfavorable conditions (Bowman 2015; Takeuchi 2016; Kalyuzhnaya 2017) and some have a flexible metabolism and are only considered facultative methanotrophs. For example, *Methylocystis* counts some taxa that can use acetate as a source of energy instead of CH₄ (Bowman 2015).

2.4.3 Negligible CH₄ concentrations in winter

In the fall, the hypolimnion had higher concentrations of CO₂ (476.45 μM, year average was 89.7 μM) and CH₄ (103.25 μM, year average was 0.4 μM), remaining as summer storage. While CO₂ diffused in the atmosphere through the mixing, CH₄ was either slower to evacuate as evidenced by the more stable concentrations into the ice-covered period, or still produced in great amounts in the surface which could be attributed to aerobic CH₄ production in terrestrial plants (Keppler *et al.* 2006). The slow decrease of CH₄ from December to January beginning by the hypolimnion implies that there was no renewal of production in the sediments from methanogenesis. This may have been caused by decreasing temperatures (Figure 4), which may impede the final enzyme of the methanogenesis reaction (MCR), sensitive to cold (Hotchkiss et DelSontro 2023).

Since ice formed before CH₄ was vented from the water column, methanotrophs may have oxidized it; however, no significant increase of CO₂ was observed at the same period. The overall decrease of CO₂ and CH₄ in the sediments after fall mixing could be due to a slower

metabolism due to colder temperatures or a reduced carbon mineralization (Liikanen *et al.* 2003) taking place when food sources are exhausted and scarcer.

In both early and late winter, CH₄ concentrations were negligible in the water column (except for surface water in December) compared to the fall and the spring. This contradicts the hypothesis of CH₄ accumulating and supersaturating in water under ice throughout winter (Juutinen *et al.* 2009; Bertilsson *et al.* 2013; Bussmann *et al.* 2021; Li et Xue 2021) and increasing when oxygen availability becomes limiting (Juutinen *et al.* 2009). Indeed, Samad et Bertilsson (2017) found greater CH₄ concentrations in winter (0.29 μM) than summer (0.19 μM), as did Juutinen *et al.* (2009) who found the bottom waters of 207 lakes to have greater CH₄ concentrations in winter (median 7.94 μmol/L) than spring, summer or fall (0.1-0.27 μmol/L). However, Miettinen *et al.* (2015) did not witness an accumulation in CH₄ over winter. The absence of CH₄ accumulation in Lake Simoncouche could be due to a high rate of CH₄ oxidation by methanotrophs (but we need to consider the copy number of *pmoA* which is lower in winter, Figure 7) or it could relate to where in the lake it was produced, and through which pathway. As described in Desrosiers *et al.* (2022), the partial pressure of CH₄ in Lake Simoncouche in summer is usually higher in the littoral vegetated zones of the lake, rather than z_{\max} where our data were collected. This study also found that a significant proportion of CH₄ is emitted through the ebullition or plant-mediated CH₄ transport rather than through the diffusive pathway, and that almost no emissions occurred in the pelagic zone of the lake (Desrosiers *et al.* 2022). Since our study only measured diffusive CH₄ in the pelagic zone of the lake, our study design may have underestimated the accumulation of CH₄. The accumulation under ice could also be in the form of bubbles from the ebullition pathway rather than in diffused form, which may in turn be trapped in the ice cover as it forms (Greene *et al.* 2014; Li et Xue 2021). However, a majority of those trapped bubbles would dissolve in the water column over winter (Greene *et al.* 2014). Another possibility would be if lateral transport of CH₄ happened towards the outlet of the lake, but no measurements were made to inspect this

possibility. Then, while two out of three replicates from March to May were unfortunately lost, the general trend in our data suggests that CH₄ concentrations were greater in spring in the water column. These are probably due to methanogenesis increasing with rising temperatures, new sources of fresh algal organic matter and lateral transport of CH₄ from the littoral associated to increasing tributary flow pushing littoral waters towards the sampling spot.

In contrast, CO₂ concentrations evolved according to the accumulation hypothesis under ice cover, followed by a mass emission into the atmosphere at the ice break, decreasing the CO₂ concentration in the water column afterwards, as previously documented in Lake Simoncouche by Vachon *et al.* (2017). Their study showed that most of the annual CO₂ in Lake Simoncouche is from the hydrological inputs over the year (87%), with a higher contribution in the fall and the spring. However, in winter, the accumulation of CO₂ under the ice would be due to sediment CO₂ fluxes and pelagic organic matter mineralization (Ducharme Riel 2011). Thus, CO₂ resulting from methanotrophy and other forms of mineralization are important sources of CO₂ in winter.

2.4.4 Methanotrophy in hypoxic zones and spring peak

The detection of the gene *pmoA* via qPCR indicates the RNA copy number in the samples, suggesting active transcription at the time of sampling, given the unstable nature of the RNA molecule. For the water column most of the methanotrophic activity was detected in the spring while for the sediments it was consistent throughout sampling period. Unexpectedly, methanotrophy did not increase and spread to the entire water column during the fall mixing, even with mixing homogenizing oxygen and CH₄ through the entire water column, which could support more CH₄ oxidization (Utsumi *et al.* 1998; Borrel *et al.* 2011; Mayr *et al.* 2020). Such mixing-induced pattern was, however, observed in spring, including mid-April when oxygen increased significantly in the hypolimnion.

We expected to find the highest copy number of *pmoA* transcripts in oxic-anoxic interfaces, since methanotrophs need both oxygen and CH₄ to accomplish methanotrophy. These interfaces are found at the water and sediment boundary in the absence of stratification (during mixing), and at the thermocline during periods of stratification (Knief 2015). In early winter, we detected activity in the hypolimnion, concurrent with hypoxic conditions (< 2 mg/L) and negligible CH₄ concentrations (~0.001 mg/L). We also found evidence of *pmoA*-mediated methanotrophy in the oxygen-depleted conditions of September, when the hypolimnion was anoxic (< 1 mg/L), with a high level of CH₄ (1.66 mg/L). Yet, methanotrophy did not persist through March, when conditions were hypoxic from the bottom up to 3.4 m in the water column. During this period, gene transcripts were only detected at 0 and 3 m waters as usually expected. To explain the phenomenon, a review by Reis *et al.* (2024) showed that aerobic methanotrophs are persistently detected and active in oxygen-deficient freshwaters, and report that more research is needed to understand those mechanisms. Potential hypotheses consist of an alternative electron acceptor (through sulfate reduction or denitrification (Bertilsson *et al.* 2013)) or gas vesicles found in some methanotrophs allowing the manipulation of their buoyancy to access oxygen higher in the water column (Reis *et al.* 2024). Anaerobic methanotrophs also exist, but they are archaea and use the same enzyme as methanogens to oxidize CH₄ (Reis *et al.* 2024), hence they don't possess the *pmoA* gene and their activity cannot be included in this analysis.

Sediments consistently showed a greater abundance of *pmoA* transcripts compared to the water column throughout the study. There was an increase of activity at both mixing periods (fall and spring) and the lowest activity happened in early winter. This was expected since there is a lower concentration in CH₄ in the sediments after the fall mixing.

Our ability to compare copy numbers obtained here to other studies is limited, as we used cDNA (from RNA) as a template to quantify activity, and most other studies used DNA to quantify the gene's abundance (Kolb *et al.* 2003). Our approach has the advantage of

excluding dormant or inactive cells carrying methanotrophy-genes and presents a conservative estimate of bacterial-methanotrophy. Nonetheless, some studies based on DNA report comparable copy numbers for *pmoA*, the average for our water samples being 1.11×10^4 while Albakistani *et al.* (2022) had 2.7×10^4 cells/mL after a normalization for an estimated 2 copies per cell. In the sediments, we had 7.16×10^7 copies/mL while Lyautey *et al.* (2021) had from 2.53×10^6 to 1.29×10^7 cells/g and Rahalkar *et al.* (2009) around 2.5×10^7 cells/g. Our data suggests that using normalized DNA copy number is an appropriate predictor of gene expression through cDNA transcripts.

2.4.5 CH₄ and TN as drivers of methanotrophic activity

Copy numbers of *pmoA* were correlated positively with TN and CH₄, and negatively with O₂ through an RVI weight analysis ranking variable by AIC. Those were among the most important factors impacting methanotrophic communities and activity as listed in Knief (2015), all of them being CH₄, oxygen, nutrients (mostly copper (Semrau *et al.* 2010) and nitrogen) and temperature. According to Ho *et al.* (2013), CH₄ and nitrogen would be the strongest factors to shape methanotrophs communities, consistent with our model linking *pmoA* copy number to these variables. The need for CH₄ for methanotrophy to function is self-explanatory since it is the source of energy for methanotrophs. The same should go for oxygen, which is the electron acceptor, and it has been found to impose a plateau for methanotrophy when limited (Reis *et al.* 2022), but also an inhibitory effect when too high (Thottathil *et al.* 2019). As discussed previously, most of the methanotrophic activity in this study prior to spring was restricted to hypoxic habitats, supporting observations among type I methanotrophs (Reis *et al.* 2024). To explain this, some taxa identified from the type I methanotrophs had genes for denitrification, a fermentation mode (Reis *et al.* 2022) or oxygen carriers like bacteriohemerythrins (Reis *et al.* 2024). If some methanotrophs have the ability to denitrify or nitrify nitrogen by using it as an electron acceptor (Dedysh et Knief 2018; Reis *et al.* 2024),

this may impact TN concentrations in the water column. However, the relation between methanotrophs and nitrogen is complex, as the addition of ammonium has been found to either inhibit or enhance methanotrophic activity (Semrau *et al.* 2010). In our study, a strong positive correlation was established with TN, suggesting that a large part of it could be from NO₂ or NO₃ which are required as an energy source for denitrifying bacteria.

Another RVI analysis was carried out to explain *pmoA* copy number by the taxonomic groups of methanotrophs that were detected in V3-V4 16S sequencing. It was separated in two analyses, one for the water and one for the sediments, since the number of copies in the sediments was of three orders of magnitude greater than in the water and biased the overall result. *Methylobacter* had a larger weight in both analyses, as it was more abundant throughout the study. Many taxa within this genus have been described in the literature and present different metabolic abilities: some are psychrophilic or psychrotolerant (*Methylobacter tundripaludum* or *Methylobacter psychrophilus*), most can form cysts (Dedysh et Knief 2018), and they are usually motile, which means they can move through the water column to ingest DO and CH₄ (Kalyuzhnaya 2017). In our model, *Methyloferula* has a negative 28% weight in the analysis, however, this is one of the two groups of methanotrophs which use a soluble monooxygenase instead of the particulate one (Ho *et al.* 2013; Dedysh *et al.* 2015; Dedysh et Knief 2018), hence its activity is not captured by the copy number of the *pmoA* gene. Other negative relationships with *pmoA* copy number found with *Candidatus Methylacidiphilum* and *Methylocystis* are due to them being more present in the fall, when the fewest *pmoA* copies were detected. The *Methylocystis* genus also presents a negative relation to *pmoA* in sediments, although it is usually found in freshwater sediments and has a temperature range of survival between 5 and 40 °C (Bowman 2015). It can also form cysts, which could bias the analysis with a non-active presence. They use acetate in the absence of CH₄ (Bowman 2015), which means they may be present and active, but oxidizing CH₄ via another enzyme.

2.4.6 Methanotrophy in lake ice

While the focus of this study was the seasonal variation of GHG and methanotrophs within a freshwater lake, ice cores collected over winter showed surprising results. To our knowledge, no study found evidence of potential methanotrophy in lake ice. Lake ice does not possess brine channels like sea ice for microbial activity to concentrate (Krembs *et al.* 2000), and has long been considered too dense to harbor active organisms (Bondarenko *et al.* 2012). However, there is growing evidence for the presence of active microbial organisms in ice, as previously described in Lake Simoncouche (Kivilä *et al.* 2023). Gas bubbles like CH₄ (Jansen *et al.* 2021) could potentially create a microhabitat, in which microbes are trapped into when ice is thickening, and support microbial activity. Since our study found cDNA copies of *pmoA* in lake ice collected in February and April (up to 1.67x10⁴ copies/mL in February and 1.01x10⁴ in April), this could suggest that methanotrophy is taking place in this specific environment. Alternatively, ice may conserve RNA more efficiently, and cDNA detected here may have simply been included from the water column as ice formed. Unfortunately, we did not stratify ice samples by layers, limiting our ability to confirm the origin of these transcripts. Higher conservation of trapped RNA would mean this happened in the black ice layer. Somehow, the environmental factor that coincides all those sampling would be water availability. February is the only month where the snow cover included a slush layer (14 cm) and in April, the snow cover was melting. Both events could induce water by percolation in the microhabitats of the ice cover, and this would mean the RNA was present in the white layer of the ice. However, the weight of the snow and the slush on the ice could squeeze the water upwards and infiltrate water in all ice layers.

Two trends were identified in the relative abundance of methanotrophs in lake ice. *Methylobacter* increased in late winter as it did in the water, so they were probably included as the ice formed. However, the second trend is the presence of *Candidatus Methylacidiphilum* in April, which was not observed in the water at this time but was in the fall. Either it could have

been included in the fall and undetected until April, or it could come from the atmosphere, the snow melting on top of the ice influencing the ice communities and sheltering some methanotrophs.

2.4.7 Conclusion

In this study, limnological data, GHG concentrations, microbial communities and methanotrophic activity were characterized a 9-month period, in winter and shoulder seasons, to get a fuller picture of methanotrophy under-ice. This is essential as ice cover limits the emissions of CH₄ and allows more chances for it to be oxidized by methanotrophs. We found that ice cover impacts microbial communities over all the water column, beginning by the epilimnion, down to the hypolimnion. Dissolved CH₄ decreased to a negligible amount in the water column, and it was one of the most important factors explaining methanotrophic activity, along with TN and followed by DO. Overall, methanotrophs sequences accounted for a low relative abundance and were dominated by *Methylobacter*. In the water column, its relative abundance increased in winter and spring, while *Candidatus Methyloacidiphilum* peaked in the fall. During winter, methanotrophic activity occurred more frequently in hypoxic zones, while highest activities were detected throughout all the water column in spring. In sediments, methanotrophy happened continuously throughout the sampling period with a temporary decrease of copy number in early winter. Sediments were more stable in terms of taxonomy and were dominated by *Methylobacter*, *Methyloparacoccus* and *Methylocystis*. Methanotrophic activity was detected in the ice as well, with a microbial composition similar to the water habitat. This study supports the idea that methanotrophic activity dominantly takes place in hypoxic zones but is more intense in presence of oxygen if CH₄ concentrations are high enough.

CHAPITRE 3 : Conclusion générale

Les changements climatiques mènent à des hivers plus chauds et plus courts, ce qui a des conséquences profondes sur le couvert de glace. Si l'hiver est une saison historiquement sous-étudiée, on comprend maintenant mieux son importance dans le régime de la lumière, d'oxygène et de GES dans les lacs. Comprendre l'effet de l'hiver dans le cycle lacustre du carbone est essentiel pour mieux prédire le rôle des lacs boréaux comme émetteurs de GES. Ainsi, l'objectif de ce mémoire était de réaliser une étude temporelle incluant l'hiver sur les microorganismes lacustres impliqués dans le cycle du CH₄. À l'aide de données physicochimiques, de mesures du CH₄ et le CO₂ dissous, de séquences du gène de l'ARNr 16S et de quantifications de l'expression du gène *pmoA* obtenues par qPCR, nous avons pu identifier les déterminants de l'activité méthanotrophe et comment l'hiver peut la moduler.

Conformément à nos attentes, les résultats soutiennent que la présence du couvert de glace en hiver impacte la colonne d'eau au niveau de la température et de l'oxygène, ce qui a mené à la sous-division de 4 saisons au fil de notre étude (automne, début de l'hiver, fin de l'hiver, printemps). Certains nutriments n'étaient pas stables au cours de la période de suivi : le DOC a diminué pendant l'hiver, tandis que le TN a augmenté. Alors que le CO₂ s'est accumulé sous la glace pendant l'hiver, le CH₄ a été détecté en quantités négligeables. Le CH₄, de pair avec le TN, fait partie des paramètres qui expliquent le mieux l'activité méthanotrophe mesurée dans l'étude. L'activité méthanotrophe a été détectée plus fréquemment dans les zones hypoxiques du lac, soit l'hypolimnion en hiver ou la surface des sédiments, ce qui soutient diverses observations récentes où les méthanotrophes démontrent des capacités alternatives de se procurer le CH₄ (Reis *et al.* 2024). L'activité méthanotrophe la plus intense a été mesurée au printemps dans toute la colonne d'eau, lorsque le brassage redistribue l'oxygène, le CH₄ et les nutriments à travers le lac. Les méthanotrophes qui dominaient l'eau et les sédiments appartenaient à des groupes différents, et dans le cas de la colonne d'eau, variaient dans le

temps. Dans l'eau, *Candidatus Methyloacidiphilum* dominait à l'automne, alors qu'en hiver ce taxon était remplacé par *Methylobacter*, un genre bactérien présentant diverses adaptations psychrophiles et psychrotolérantes (Kalyuzhnaya 2017). Les sédiments présentaient trois groupes dominants et stables au fil de la saison d'échantillonnage, soient *Methylobacter*, *Methyloparacoccus* et *Methylocystis*. Une observation surprenante de l'étude fut la découverte de transcrits d'ARN du gène *pmoA* dans la glace du lac à deux reprises au fil de l'hiver, soit en février et en avril, ce qui n'avait jamais été répertorié auparavant. Les transcrits d'ARN indiquent habituellement une activité du gène en question. Toutefois étant dans la glace, il est possible que ces transcrits aient été incorporés depuis la colonne d'eau au moment du gel et conservés dans la glace, et indiquent plutôt une activité sous la glace pendant la formation du couvert.

Il est important de reconnaître que notre étude présente quelques limites. Notamment, nous n'avons pas d'informations sur l'origine des gaz mesurés. Par exemple, quelle est la proportion de CO₂ qui provient de la méthanotrophie ? Est-ce que le méthane n'est produit que par la méthanogénèse dans les sédiments, où y a-t-il de la production en milieu aérobie ? Pour répondre à ces questions, il aurait été intéressant de réaliser des analyses d'isotopes stables sur les échantillons de gaz afin de déterminer leur origine. Également, cette étude ne présente que les gaz dissous dans la colonne d'eau et les sédiments, et ne tient pas compte du CH₄ issu de l'ébullition, un processus déjà documenté dans le lac Simoncouche (Desrosiers *et al.* 2022). Les approches de mesures d'ébullition sont bien développées pour les conditions d'eau libre (par chambres flottantes déployées à la surface de l'eau), et plus complexes pour la saison de couvert de glace. Il aurait été intéressant d'adapter les chambres flottantes traditionnellement utilisées pour capter le CH₄ en ébullition à l'hiver, car, bien que peu biodisponible pour les microorganismes, cette forme du CH₄ est un vecteur important d'émissions vers l'atmosphère dans les lacs boréaux. Une autre limite de l'étude est que notre collecte d'échantillons était restreinte au point le plus profond du lac, omettant ainsi le littoral, qui recouvre une aire

beaucoup plus importante d'un lac peu profond comme Simoncouche et présente des conditions différentes. D'abord, en zones peu profondes, la colonne d'eau est moins épaisse et il y a moins de possibilités pour que les méthanotrophes captent le CH₄. Il y a également moins de chance que ces zones du lac soient stratifiées et présentent un hypolimnion, où le CH₄ s'accumule habituellement. Ensuite, puisque la lumière est plus à même d'atteindre le fond du lac, les végétaux peuvent s'installer dans le milieu benthique et oxygéner la colonne d'eau via la photosynthèse. De plus, avec la lumière, la température de l'eau est plus élevée jusqu'aux sédiments : puisque les méthanogènes sont sensibles au froid, leur activité peut y être élevée en été. Par contre, elle risque d'être plus faible en hiver, car la stratification inverse n'y permettra pas des conditions similaires à l'hypolimnion. L'étude de Desrosiers *et al.* (2022) a déjà répertorié que les voies d'émissions du CH₄ sont plus diversifiées au niveau du littoral dans le lac Simoncouche. En effet, si la méthanogénèse est plus intense, le CH₄ s'accumule dans les sédiments et forme des bulles avant de se rendre dans la colonne d'eau. De plus, avec la présence des végétaux, le CH₄ peut également emprunter la voie de transport médié par les plantes pour se rendre dans l'atmosphère. Bref, il aurait été intéressant d'échantillonner divers points pour effectuer des conclusions plus fortes à l'égard de la totalité du lac. Par ailleurs, le lac Simoncouche n'est qu'un seul lac et plus d'études avec une résolution temporelle aussi fine seront nécessaires pour confirmer et généraliser sur des échelles spatiales plus grandes les phénomènes que nous rapportons. Finalement, afin de déterminer précisément de quels organismes venait l'activité méthanotrophe, le séquençage de l'ARN du gène *pmoA* aurait été intéressant : il aurait été possible d'associer chaque transcrit d'ARN (donc gène actif) au taxon méthanotrophe spécifique qui l'a produit, tout en explorant la diversité génomique de cette voie métabolique importante. Cela pourrait confirmer l'implication des *Methylobacter* dans la méthanotrophie hivernale d'une manière plus directe que les RVI qui ont été effectuées dans la présente étude (Figure 8). Malgré ces limites, notre étude permet tout de même d'explorer la méthanotrophie en milieu lacustre hivernal sous une résolution mensuelle.

En conclusion, cette recherche contribue à la compréhension de la dynamique hivernale des lacs boréaux et plus spécifiquement à nos connaissances sur la diversité et à l'activité des méthanotrophes qui oxydent le CH₄ en CO₂. Ceci est nécessaire vu les projections climatiques actuelles au niveau du Canada : en effet, les températures hivernales de l'air ont en moyenne augmenté de 3,6 °C depuis les 77 dernières années (Environnement et Changement climatique Canada 2024), ce qui a un impact inévitable sur la durée des couverts de glace sur les lacs. Le rôle des lacs boréaux dans le cycle des GES changera donc probablement au cours des prochaines décennies par la perte du couvert de glace qui permet d'emprisonner le CH₄ en attendant son oxydation par les méthanotrophes, mais également au niveau d'autres processus hivernaux qui demeurent mal compris en raison de l'importance relativement nouvelle que l'on accorde à cette saison. En considérant la détection de la méthanotrophie hivernale en milieu hypoxique dans la présente étude, une formation de la glace tardive ou un dégel précoce pourraient également affecter les microorganismes méthanotrophes dans le lac Simoncouche. En effet, avec des hivers plus courts qui limitent moins la disponibilité en oxygène dans le lac, l'habitat de ces microorganismes serait amené à changer, ce qui pourrait limiter la probabilité d'oxydation du méthane, augmentant la concentration du gaz dans le lac au moment du dégel. Ainsi, il est critique de poursuivre les études en limnologie hivernale : les microorganismes n'y sont pas en dormance, contrairement à ce qui a été cru pendant trop longtemps, ils sont plutôt actifs et la présente étude en est une démonstration claire. Également, le métabolisme de microorganismes tels que les méthanotrophes semble être bien connu en été, mais présentent ici une stratégie divergente en conditions hivernales (besoins en oxygène). L'hiver est une période centrale dans le rôle d'un lac à l'échelle du paysage, ainsi il ne tarde d'en apprendre le plus possible avant qu'il ne soit trop tard et que les hivers tels qu'on les connaît ne disparaissent en raison du réchauffement.

Liste de références

Albakistani EA, Nwosu FC, Furgason C, Haupt ES, Smirnova AV, Verbeke TJ, Lee ES, Kim JJ, Chan A, Ruhl IA, Sheremet A, Rudderham SB, Lindsay MJB et Dunfield PF. 2022. Seasonal dynamics of methanotrophic bacteria in a boreal oil sands end pit lake. *Applied and Environmental Microbiology*, 88 : e0145521.

Bartoń K. 2024. MuMIn: Multi-model inference v.1.48.4. <https://cran.r-project.org/web/packages/MuMIn/MuMIn.pdf>

Bastviken D, Ejlertsson J et Tranvik L. 2002. Measurement of methane oxidation in lakes: A comparison of methods. *Environmental Science & Technology*, 36 : 3354-3361.

Bastviken D, Cole J, Pace M et Tranvik L. 2004. Methane emissions from lakes: Dependence of lake characteristics, two regional assessments, and a global estimate. *Global Biogeochemical Cycles*, 18 : GB4009.

Bertilsson S, Burgin A, Carey C, Fey S, Grossart H-P, Grubisic L, Jones I, Kirillin G, Lennon J, Shade A et Smyth R. 2013. The under-ice microbiome of seasonally frozen lakes. *Limnology and Oceanography*, 58 : 1998-2012.

Bizic-Ionescu M, Amann R et Grossart HP. 2014. Massive regime shifts and high activity of heterotrophic bacteria in an ice-covered lake. *PLoS ONE*, 9 : e113611.

Block BD, Denfeld BA, Stockwell JD, Flaim G, Grossart H-PF, Knoll LB, Maier DB, North RL, Rautio M, Rusak JA, Sadro S, Weyhenmeyer GA, Bramburger AJ, Branstrator DK, Salonen K et Hampton SE. 2019. The unique methodological challenges of winter limnology. *Limnology and oceanography: Methods*, 17 : 42-57.

Bondarenko NA, Belykh OI, Golobokova LP, Artemyeva OV, Logacheva NF, Tikhonova IV, Lipko IA, Kostornova TY, Parfenova VV, Khodzher TV, Ahn TS et Zo YG. 2012. Stratified distribution of nutrients and extremophile biota within freshwater ice covering the surface of Lake Baikal. *Journal of Microbiology*, 50 : 8-16.

Borrel G, Jezequel D, Biderre-Petit C, Morel-Desrosiers N, Morel JP, Peyret P, Fonty G et Lehours AC. 2011. Production and consumption of methane in freshwater lake ecosystems. *Research in Microbiology*, 162 : 832-847.

Bowman J. 2015. *Methylocystis*. Dans : Whitman WB éd. *Bergey's manual of systematics of archaea and bacteria*. John Wiley & Sons, Inc., Hoboken, New Jersey.

Bowman Jr. LL. 2015. *Methylococcus*. Dans : Whitman WB éd. *Bergey's manual of systematics of archaea and bacteria*. John Wiley & Sons, Inc., Hoboken, New Jersey.

Boyce FM. 2006 (mis à jour le 2024/30/04). Lakes in Canada. Consulté le 19 juin, <https://www.thecanadianencyclopedia.ca/en/article/lake#:~:text=Canada%20has%20a%20many%20as,Lake%20Huron%2C%20and%20Lake%20Erie>.

- Buchan A, LeCleir GR, Gulvik CA et Gonzalez JM. 2014. Master recyclers: Features and functions of bacteria associated with phytoplankton blooms. *Nature Reviews Microbiology*, 12 : 686-698.
- Bussmann I, Fedorova I, Juhls B, Overduin PP et Winkel M. 2021. Methane dynamics in three different Siberian water bodies under winter and summer conditions. *Biogeosciences*, 18 : 2047-2061.
- Butler TM, Wilhelm A-C, Dwyer AC, Webb PN, Baldwin AL et Techtmann SM. 2019. Microbial community dynamics during lake ice freezing. *Scientific Reports*, 9 : 6231.
- Callahan BJ, McMurdie PJ, Rosen MJ, Han AW, Johnson AJ et Holmes SP. 2016. DADA2: High-resolution sample inference from Illumina amplicon data. *Nature methods*, 13 : 581-583.
- Capo E, Rydberg J, Tolu J, Domaizon I, Debroas D, Bindler R et Bigler C. 2019. How does environmental inter-annual variability shape aquatic microbial communities? A 40-year annual record of sedimentary DNA from a boreal lake (Nylandssjön, Sweden). *Frontiers in Ecology and Evolution*, 7 : 1-13.
- Catalan J. 1992. Evolution of dissolved and particulate matter during the Ice-covered period in a deep, high-mountain lake. *Canadian Journal of Fisheries and Aquatic Sciences*, 49 : 945-955.
- Cavaliere E et Baulch HM. 2021. Winter in two phases: Long-term study of a shallow reservoir in winter. *Limnology and Oceanography*, 66 : 1335-1352.
- Cavaliere E, Fournier IB, Hazuková V, Rue GP, Sadro S, Berger SA, Cotner JB, Dugan HA, Hampton SE, Lottig NR, McMeans BC, Ozersky T, Powers SM, Rautio M et O'Reilly CM. 2021. The lake ice continuum concept: Influence of winter conditions on energy and ecosystem dynamics. *Journal of Geophysical Research: Biogeosciences*, 126.
- Chan CN, Gushulak CAC, Leavitt PR, Logozzo LA, Finlay K et Bogard MJ. 2024. Experimental ecosystem eutrophication causes offsetting effects on emissions of CO₂, CH₄, and N₂O from agricultural reservoirs. *Environmental Science & Technology*, 58 : 7045-7055.
- Cole JJ, Prairie YT, Caraco NF, McDowell WH, Tranvik LJ, Striegl RG, Duarte CM, Kortelainen P, Downing JA, Middelburg JJ et Melack J. 2007. Plumbing the global carbon cycle: Integrating inland waters into the terrestrial carbon budget. *Ecosystems*, 10 : 172-185.
- Cortés A, MacIntyre S et Sadro S. 2017. Flowpath and retention of snowmelt in an ice-covered Arctic lake. *Limnology and Oceanography*, 62 : 2023-2044.

Costello AM et Lidstrom ME. 1999. Molecular characterization of functional and phylogenetic genes from natural populations of methanotrophs in lake sediments. *Applied and Environmental Microbiology*, 65 : 5066-5074.

Cruaud P, Vigneron A, Fradette M-S, Charette SJ, Rodriguez MJ, Dorea CC et Culley AI. 2017. Open the Sterivex™ casing: an easy and effective way to improve DNA extraction yields. *Limnology and oceanography: Methods*, 15 : 1015-1020.

Dedysh S et Knief C. 2018. Diversity and phylogeny of described aerobic methanotrophs. Dans : Kalyuzhnaya MG et Xing X-H éd. *Methane Biocatalysis: Paving the Way to Sustainability*. Springer, Cham, Cham, Switzerland, p. 17-42.

Dedysh SN, Liesack W, Khmelenina VN, Suzina NE, Trotsenko YA, Semrau JD, Bares AM, Panikov NS et Tiedje JM. 2000. *Methylocella palustris* gen. nov., sp. nov., a new methane-oxidizing acidophilic bacterium from peat bogs, representing a novel subtype of serine-pathway methanotrophs. *International Journal of Systematic and Evolutionary Microbiology*, 50 : 955-969.

Dedysh SN, Naumoff DG, Vorobev AV, Kyrpides N, Woyke T, Shapiro N, Crombie AT, Murrell JC, Kalyuzhnaya MG, Smirnova AV et Dunfield PF. 2015. Draft genome sequence of *Methyloferula stellata* AR4, an obligate methanotroph possessing only a soluble methane monooxygenase. *Genome Announcements*, 3 : e01555-01514.

Denfeld B, Klaus M, Laudon H, Sponseller R et Karlsson J. 2018a. Carbon dioxide and methane dynamics in a small boreal lake during winter and spring melt events. *Journal of Geophysical Research: Biogeosciences*, 123 : 2527-2540.

Denfeld BA, Baulch HM, del Giorgio PA, Hampton SE et Karlsson J. 2018b. A synthesis of carbon dioxide and methane dynamics during the ice-covered period of northern lakes. *Limnology and Oceanography Letters*, 3 : 117-131.

Desrosiers K, DelSontro T et del Giorgio PA. 2022. Disproportionate contribution of vegetated habitats to the CH₄ and CO₂ budgets of a boreal lake. *Ecosystems*, 25 : 1522-1541.

Ducharme Riel V. 2011. Dynamique hivernale et hypolimnétique du CO₂ dans les lacs boréaux et tempérés. Mémoire de maîtrise, Université du Québec à Montréal, Montréal, 116 p.

Dunfield PF, Yuryev A, Senin P, Smirnova AV, Stott MB, Hou S, Ly B, Saw JH, Zhou Z, Ren Y, Wang J, Mountain BW, Crowe MA, Weatherby TM, Bodelier PLE, Liesack W, Feng L, Wang L et Alam M. 2007. Methane oxidation by an extremely acidophilic bacterium of the phylum Verrucomicrobia. *Nature*, 450 : 879-882.

Environment and Climate Change Canada. 2024. Canadian climate normals 1991-2020 data, station: Bagotville. Consulté le 29 août 2024, https://climate.weather.gc.ca/climate_normals/results_1991_2020_e.html?searchType=stnProx&txtRadius=25&selCity=&selPark=&txtCentralLatDeg=48&txtCentralLatMin=23&txtCentralLatSec=0&txtCentralLongDeg=71&txtCentralLongMin=25&txtCentralLongSec=0&optProxType=decimal&txtLatDecDeg=48.23&txtLongDecDeg=-71.25&stnID=83000000&dispBack=0

Environnement et Changement climatique Canada. 2024 (mis à jour le 2024/05/03). Bulletin des tendances et des variations climatiques – Hiver 2023-2024. Consulté le 21 juin, <https://www.canada.ca/fr/environnement-changement-climatique/services/changements-climatiques/recherche-donnees/tendances-variabilite-climatiques/tendances-variations/bulletin-hiver-2024.html>

Fallon RD, Harrits S, Hanson RS et Brock TD. 1980. The role of methane in internal carbon cycling in Lake Mendota during summer stratification. *Limnology and Oceanography*, 25 : 357-360.

Forrest A, Andradóttir H et Laval B. 2011. Preconditioning of an underflow during ice-breakup in a subarctic lake. *Aquatic Sciences*, 74 : 361–374.

Frenzel P, Thebrath B et Conrad R. 1990. Oxidation of methane in the oxic surface layer of a deep lake sediment (Lake Constance). *FEMS Microbiology Ecology*, 6 : 149-158.

Gouvernement du Canada. 2023 (mis à jour le 2023-06-29). Greenhouse gas concentrations. Consulté le 05 juin, <https://www.canada.ca/en/environnement-climate-change/services/environmental-indicators/greenhouse-gas-concentrations.html>

Greene S, Walter Anthony KM, Archer D, Sepulveda-Jauregui A et Martinez-Cruz K. 2014. Modeling the impediment of methane ebullition bubbles by seasonal lake ice. *Biogeosciences*, 11 : 6791-6811.

Hampton SE, Galloway AW, Powers SM, Ozersky T, Woo KH, Batt RD, Labou SG, O'Reilly CM, Sharma S, Lottig NR, Stanley EH, North RL, Stockwell JD, Adrian R, Weyhenmeyer GA, Arvola L, Baulch HM, Bertani I, Bowman LL, Jr., Carey CC, Catalan J, Colom-Montero W, Domine LM, Felip M, Granados I, Gries C, Grossart HP, Haberman J, Haldna M, Hayden B, Higgins SN, Jolley JC, Kahilainen KK, Kaup E, Kehoe MJ, MacIntyre S, Mackay AW, Mariash HL, McKay RM, Nixdorf B, Noges P, Noges T, Palmer M, Pierson DC, Post DM, Pruett MJ, Rautio M, Read JS, Roberts SL, Rucker J, Sadro S, Silow EA, Smith DE, Sterner RW, Swann GE, Timofeyev MA, Toro M, Twiss MR, Vogt RJ, Watson SB, Whiteford EJ et Xenopoulos MA. 2017. Ecology under lake ice. *Ecology Letters*, 20 : 98-111.

Hanson RS et Hanson TE. 1996. Methanotrophic bacteria. *Microbiological Reviews*, 60 : 439-471.

Hébert M-P, Beisner BE, Rautio M et Fussmann GF. 2021. Warming winters in lakes: Later ice onset promotes consumer overwintering and shapes springtime planktonic food webs. *Proceedings of the National Academy of Sciences*, 118 : e2114840118.

Helms JR, Stubbins A, Ritchie JD, Minor EC, Kieber DJ et Mopper K. 2008. Absorption spectral slopes and slope ratios as indicators of molecular weight, source, and photobleaching of chromophoric dissolved organic matter. *Limnology and Oceanography*, 53 : 955-969.

Herlemann DP, Labrenz M, Jürgens K, Bertilsson S, Waniek JJ et Andersson AF. 2011. Transitions in bacterial communities along the 2000 km salinity gradient of the Baltic Sea. *The ISME Journal*, 5 : 1571-1579.

Ho A, Kerckhof FM, Luke C, Reim A, Krause S, Boon N et Bodelier PL. 2013. Conceptualizing functional traits and ecological characteristics of methane-oxidizing bacteria as life strategies. *Environmental Microbiology Reports*, 5 : 335-345.

Hotchkiss E et DelSontro T. 2023. Organic carbon cycling and ecosystem metabolism. Dans : Jones I et Smol J éd. *Wetzel's Limnology Lake and River Ecosystems Fourth Edition* Academic Press, Elsevier, Cambridge, USA.

Imbeau E, Vincent WF, Wauthy M, Cusson M et Rautio M. 2021. Hidden stores of organic matter in northern lake ice: Selective retention of terrestrial particles, phytoplankton and labile carbon. *Journal of Geophysical Research: Biogeosciences*, 126 : e2020JG006233.

Imrit MA et Sharma S. 2021. Climate change is contributing to faster rates of lake ice loss in lakes around the northern hemisphere. *Journal of Geophysical Research: Biogeosciences*, 126 : e2020JG006134.

Ivanova AA, Philippov DA, Kulichevskaya IS et Dedysh SN. 2018. Distinct diversity patterns of *Planctomycetes* associated with the freshwater macrophyte *Nuphar lutea* (L.) Smith. *Antonie van Leeuwenhoek*, 111 : 811-823.

Jansen J, MacIntyre S, Barrett DC, Chin YP, Cortés A, Forrest AL, Hrycik AR, Martin R, McMeans BC, Rautio M et Schwefel R. 2021. Winter limnology: How do hydrodynamics and biogeochemistry shape ecosystems under ice? *Journal of Geophysical Research: Biogeosciences*, 126 : e2020JG006237.

Jones I et Smol J. 2023. *Wetzel's limnology: Lake and river ecosystems*, 4th ed. Elsevier Science, Amsterdam, 1104 p.

Juottonen H, Fontaine L, Wurzbacher C, Drakare S, Peura S et Eiler A. 2020. Archaea in boreal Swedish lakes are diverse, dominated by Woese archaeota and follow deterministic community assembly. *Environmental Microbiology*, 22 : 3158-3171.

Juutinen S, Rantakari M, Kortelainen P, Huttunen JT, Larmola T, Alm J, Silvola J et Martikainen PJ. 2009. Methane dynamics in different boreal lake types. *Biogeosciences*, 6 : 209-223.

Kalyuzhnaya M. 2017. *Methylobacter*. Dans : Whitman WB éd. *Bergey's manual of systematics of archaea and bacteria*. John Wiley & Sons, Inc., Hoboken, New Jersey.

Kankaala P, Huotari J, Peltomaa E, Saloranta T et Ojala A. 2006. Methanotrophic activity in relation to methane efflux and total heterotrophic bacterial production in a stratified, humic, boreal lake. *Limnology and Oceanography*, 51 : 1195-1204.

Kassambara A. 2023. rstatix: Pipe-friendly framework for basic statistical tests. <https://rpkgs.datanovia.com/rstatix/>

Keppler F, Hamilton JTG, Braß M et Röckmann T. 2006. Methane emissions from terrestrial plants under aerobic conditions. *Nature*, 439 : 187-191.

Kivilä EH, Prėskienis V, Gaudreault N, Girard C et Rautio M. 2023. Variability in lake bacterial growth and primary production under lake ice: Evidence from early winter to spring melt. *Limnology and Oceanography*, 68 : 2603-2616.

Knief C. 2015. Diversity and habitat preferences of cultivated and uncultivated aerobic methanotrophic bacteria evaluated based on *pmoA* as molecular marker. *Frontiers in Microbiology*, 6 : 1346.

Kolb S, Knief C, Stubner S et Conrad R. 2003. Quantitative detection of methanotrophs in soil by novel *pmoA*-targeted real-time PCR assays. *Applied and Environmental Microbiology*, 69 : 2423-2429.

Korver MC, Lehner B, Cardille JA et Carrea L. 2024. Surface water temperature observations and ice phenology estimations for 1.4 million lakes globally. *Remote Sensing of Environment*, 308 : 114164.

Kotsyurbenko OR, Chin KJ, Glagolev MV, Stubner S, Simankova MV, Nozhevnikova AN et Conrad R. 2004. Acetoclastic and hydrogenotrophic methane production and methanogenic populations in an acidic West-Siberian peat bog. *Environmental Microbiology*, 6 : 1159-1173.

Krembs C, Gradinger R et Spindler M. 2000. Implications of brine channel geometry and surface area for the interaction of sympagic organisms in Arctic sea ice. *Journal of Experimental Marine Biology and Ecology*, 243 : 55-80.

Kulichevskaya IS, Naumoff DG, Miroshnikov KK, Ivanova AA, Philippov DA, Hakobyan A, Rijpstra WIC, Damsté JSS, Liesack W et Dedysh SN. 2020. *Limnoglobus roseus* gen. nov., sp. nov., a novel freshwater *planctomycete* with a giant genome from the family *Gemmataceae*. *International Journal of Systematic and Evolutionary Microbiology*, 70 : 1240-1249.

Lepistö A, Futter MN et Kortelainen P. 2014. Almost 50 years of monitoring shows that climate, not forestry, controls long-term organic carbon fluxes in a large boreal watershed. *Global Change Biology*, 20 : 1225-1237.

Leppäranta M. 2015. Freezing of lakes and the evolution of their ice cover. Springer, Berlin, Allemagne, 311 p.

Li L et Xue B. 2021. Methane emissions from northern lakes under climate change: A review. *SN Applied Sciences*, 3 : 883.

Li X, Meng Z, Chen K, Hu F, Liu L, Zhu T et Yang D. 2023. Comparing diversity patterns and processes of microbial community assembly in water column and sediment in Lake Wuchang, China. *PeerJ*, 11 : e14592.

Liikanen A, Huttunen J, Murtoniemi T, Tanskanen H, Vaisanen T, Silvola J, Alm J et Martikainen P. 2003. Spatial and seasonal variation in greenhouse gas and nutrient dynamics and their interactions in sediments of a boreal eutrophic lake. *Biogeochemistry*, 65 : 83-103.

Linz AM, He S, Stevens SLR, Anantharaman K, Rohwer RR, Malmstrom RR, Bertilsson S et McMahon KD. 2018. Freshwater carbon and nutrient cycles revealed through reconstructed population genomes. *PeerJ*, 6 : e6075.

Lyautey E, Billard E, Tissot N, Jacquet S et Domaizon I. 2021. Seasonal dynamics of abundance, structure, and diversity of methanogens and methanotrophs in lake sediments. *Microbial Ecology*, 82 : 559-571.

Martin G, Rissanen AJ, Garcia SL, Mehrshad M, Buck M et Peura S. 2021. *Candidatus Methyllumidiphilus* drives peaks in methanotrophic relative abundance in stratified lakes and ponds across northern landscapes. *Frontiers in Microbiology*, 12 : 669937.

Mayr MJ, Zimmermann M, Guggenheim C, Brand A et Bürgmann H. 2019. Niche partitioning of methane-oxidizing bacteria along the oxygen–methane counter gradient of stratified lakes. *The ISME Journal*, 14 : 274-287.

Mayr MJ, Zimmermann M, Dey J, Brand A, Wehrli B et Bürgmann H. 2020. Growth and rapid succession of methanotrophs effectively limit methane release during lake overturn. *Communications Biology*, 3 : 108.

McMurdie PJ et Holmes S. 2013. phyloseq: an R package for reproducible interactive analysis and graphics of microbiome census data. *PLoS ONE*, 8 : e61217.

Miettinen H, Pumpanen J, J. HJ, Aaltonen H, Mammarella I, Ojala A, Levula J et Rantakari M. 2015. Towards a more comprehensive understanding of lacustrine greenhouse gas dynamics — two-year measurements of concentrations and fluxes of CO₂, CH₄ and N₂O in a typical boreal lake surrounded by managed forests. *Boreal Environment Research*, 20 : 75-89.

Ministère des Ressources naturelles et des Forêts. 2022. Cartographie du 5e inventaire écoforestier du Québec méridional—méthodes et données associées. Consulté le 29 août 2024, <https://www.donneesquebec.ca/recherche/dataset/carte-ecoforestiere-avec-perturbations>

Morris SA, Radajewski S, Willison TW et Murrell JC. 2002. Identification of the functionally active methanotroph population in a peat soil microcosm by stable-isotope probing. *Applied and Environmental Microbiology*, 68 : 1446-1453.

Oksanen FJ, Blanchet FG, Friendly M, Kindt R, Legendre P, McGlenn D, Minchin P, O'Hara RB, Simpson G et Solymos P. 2017. *vegan*: community ecology package. R package version 2.4-4. CRAN R-project.org/package=vegan.

Pernica P, North RL et Baulch HM. 2017. In the cold light of day: The potential importance of under-ice convective mixed layers to primary producers. *Inland Waters*, 7 : 138-150.

Pester M, Friedrich MW, Schink B et Brune A. 2004. *pmoA*-based analysis of methanotrophs in a littoral lake sediment reveals a diverse and stable community in a dynamic environment. *Applied and Environmental Microbiology*, 70 : 3138-3142.

Pol A, Heijmans K, Harhangi HR, Tedesco D, Jetten MS et Op den Camp HJ. 2007. Methanotrophy below pH 1 by a new *Verrucomicrobia* species. *Nature*, 450 : 874-878.

Poulin B, Ryan J et Aiken G. 2014. Effects of iron on optical properties of dissolved organic matter. *Environmental Science and Technology*, 48 : 10098-10106.

Quast C, Pruesse E, Yilmaz P, Gerken J, Schweer T, Yarza P, Peplies J et Glöckner FO. 2013. The SILVA ribosomal RNA gene database project: Improved data processing and web-based tools. *Nucleic Acids Research*, 41 : D590-D596.

R Core Team. 2021. R: A language and environment for statistical computing. <https://www.R-project.org/>

Rahalkar M, Deutzmann J, Schink B et Bussmann I. 2009. Abundance and activity of methanotrophic bacteria in littoral and profundal sediments of Lake Constance (Germany). *Applied and Environmental Microbiology*, 75 : 119-126.

Rasilo T, Prairie YT et Del Giorgio PA. 2015. Large-scale patterns in summer diffusive CH₄ fluxes across boreal lakes, and contribution to diffusive C emissions. *Global Change Biology*, 21 : 1124-1139.

Reis PCJ, Thottathil SD et Prairie YT. 2022. The role of methanotrophy in the microbial carbon metabolism of temperate lakes. *Nature Communications*, 13 : 43.

Reis PCJ, Tsuji JM, Weiblen C, Schiff SL, Scott M, Stein LY et Neufeld JD. 2024. Enigmatic persistence of aerobic methanotrophs in oxygen-limiting freshwater habitats. *The ISME Journal*, 18 : wrac041.

Rissanen A, Peura S, Mpamah P, Taipale S, Tirola M, Biasi C, Mäki A et Nykänen H. 2019. Vertical stratification of bacteria and archaea in sediments of a small boreal humic lake. *FEMS Microbiology Letters*, 366 : 1-11.

Rissanen AJ, Saarenheimo J, Tirola M, Peura S, Aalto SL, Karvinen A et Nykänen H. 2018. Gammaproteobacterial methanotrophs dominate methanotrophy in aerobic and anaerobic layers of boreal lake waters. *Aquatic Microbial Ecology*, 81 : 257-276.

Rochette P et Bertrand N. 2008. Soil-surface gas emissions. Dans : Carter MR et Gregorich E éd. *Soil sampling and methods of analysis*. CRC Press, Boca Raton, USA, p. 851–861.

Salonen K, Leppäranta M, Viljanen M et Gulati RD. 2009. Perspectives in winter limnology: closing the annual cycle of freezing lakes. *Aquatic Ecology*, 43 : 609-616.

Samad MS et Bertilsson S. 2017. Seasonal variation in abundance and diversity of bacterial methanotrophs in five temperate lakes. *Frontiers in Microbiology*, 8 : 142.

Schütte UME, Cadieux SB, Hemmerich C, Pratt LM et White JR. 2016. Unanticipated geochemical and microbial community structure under seasonal ice cover in a dilute, dimictic Arctic lake. *Frontiers in Microbiology*, 7 : 1035.

Semrau JD, DiSpirito AA et Yoon S. 2010. Methanotrophs and copper. *FEMS Microbiology Reviews*, 34 : 496-531.

Sharma S, Richardson DC, Woolway RI, Imrit MA, Bouffard D, Blagrove K, Daly J, Filazzola A, Granin N, Korhonen J, Magnuson J, Marszelewski W, Matsuzaki S-IS, Perry W, Robertson DM, Rudstam LG, Weyhenmeyer GA et Yao H. 2021. Loss of ice cover, shifting phenology, and more extreme events in northern hemisphere lakes. *Journal of Geophysical Research: Biogeosciences*, 126 : e2021JG006348.

Steinberg LM et Regan JM. 2009. mcrA-targeted real-time quantitative PCR method to examine methanogen communities. *Applied and Environmental Microbiology*, 75 : 4435-4442.

Takeuchi M. 2016. *Methylocaldum*. Dans : Whitman WB éd. *Bergey's manual of systematics of archaea and bacteria*. John Wiley & Sons, Inc., Hoboken, New Jersey.

Thottathil SD, Reis PCJ et Prairie YT. 2019. Methane oxidation kinetics in northern freshwater lakes. *Biogeochemistry*, 143 : 105-116.

Tran P, Ramachandran A, Khawasik O, Beisner BE, Rautio M, Huot Y et Walsh DA. 2018. Microbial life under ice: Metagenome diversity and in situ activity of Verrucomicrobia in seasonally ice-covered Lakes. *Environmental Microbiology*, 20 : 2568-2584.

Tsutsumi M, Kojima H et Fukui M. 2012. Vertical profiles of abundance and potential activity of methane-oxidizing bacteria in sediment of Lake Biwa, Japan. *Microbes and Environments*, 27 : 67-71.

- Tulonen T, Kankaala P, Ojala A et Arvola L. 1994. Factors controlling production of phytoplankton and bacteria under ice in a humic, boreal lake. *Journal of Plankton Research*, 16 : 1411-1432.
- Utsumi M, Nojiri Y, Nakamura T, Nozawa T, Otsuki A, Takamura N, Watanabe M et Seki H. 1998. Dynamics of dissolved methane and methane oxidation in dimictic Lake Nojiri during winter. *Limnology and Oceanography*, 43 : 10-17.
- Vachon D et del Giorgio PA. 2014. Whole-lake CO₂ dynamics in response to storm events in two morphologically different lakes. *Ecosystems*, 17 : 1338-1353.
- Vachon D, Solomon CT et del Giorgio PA. 2017. Reconstructing the seasonal dynamics and relative contribution of the major processes sustaining CO₂ emissions in northern lakes. *Limnology and Oceanography*, 62 : 706-722.
- van Grinsven S, Meier DV, Michel A, Han X, Schubert CJ et Lever MA. 2022. Redox zone and trophic state as drivers of methane-oxidizing bacterial abundance and community structure in lake sediments. *Frontiers in Environmental Science*, 10 : 857358.
- Vincent W. 2019. *Les lacs : une brève introduction*. Les Presses de l'Université Laval, Quebec, Canada, 204 p.
- Weishaar JL, Aiken GR, Bergamaschi BA, Fram MS, Fujii R et Mopper K. 2003. Evaluation of specific ultraviolet absorbance as an indicator of the chemical composition and reactivity of dissolved organic carbon. *Environmental Science & Technology*, 37 : 4702-4708.
- Wickham H. 2016. *ggplot2: elegant graphics for data analysis*. Springer-Verlag New York.
- Wickham H, François R, Henry L, Müller K et Vaughan D. 2023. *dplyr: a grammar of data manipulation*.
- Williamson CE, Saros JE et Schindler DW. 2009. Climate change. *Sentinels of change*. *Science*, 323 : 887-888.
- Xiao Y-H, Sara-Aho T, Hartikainen H et Vähätalo A. 2013. Contribution of ferric iron to light absorption by chromophoric dissolved organic matter. *Limnology and Oceanography*, 58 : 653-662.
- Yang Y, Tong T, Chen J, Liu Y et Xie S. 2020. Ammonium impacts methane oxidation and methanotrophic community in freshwater sediment. *Frontiers in Bioengineering and Biotechnology*, 8 : 250.
- Yilmaz P, Parfrey LW, Yarza P, Gerken J, Pruesse E, Quast C, Schweer T, Peplies J, Ludwig W et Glöckner FO. 2014. The SILVA and “All-species Living Tree Project (LTP)” taxonomic frameworks. *Nucleic Acids Research*, 42 : D643-D648.

Youngblut ND, Dell'aringa M et Whitaker RJ. 2014. Differentiation between sediment and hypolimnion methanogen communities in humic lakes. *Environmental Microbiology*, 16 : 1411-1423.

Zinger L, Amaral-Zettler LA, Fuhrman JA, Horner-Devine MC, Huse SM, Welch DBM, Martiny JBH, Sogin M, Boetius A et Ramette A. 2011. Global patterns of bacterial beta-diversity in seafloor and seawater ecosystems. *PLoS ONE*, 6 : e24570.

ANNEXES

ANNEXE 1 : Supplementary materials (Chapitre 2)

Supplementary methods

Method S1. PCR protocol. To confirm the primers A189F (GGNGACTGGGACTTCTGG) and mb661R (CCGGMGCAACGTCYTTACC) used in the qPCR reaction, PCR was executed in 50 μ L reactions based on the M2073 protocol (New England Biolabs, Ipswich, MA, USA): 5 μ L of sample was added to 5 μ L of Taq Reaction standard buffer, 1 μ L of dNTPs, 1 μ L of each of the primers, 0.25 μ L of Taq DNA polymerase (New England Biolabs) and 36.75 μ L of UltraPure™ nuclease-free water (Invitrogen). Genomic DNA from *Methylococcus capsulatus* strain Bath (33009, American Type Culture Collection, Manassas, VA, USA) was used for the positive control. The PCR was performed on the CFX96 Touch Real-Time PCR Detection System (Bio-Rad) with the lid at 105 °C as follows: initial denaturation for 2 minutes at 96 °C, 20 second denaturation at 96 °C, 20 second annealing at 51 °C for *pmoA* primers, and 30 second elongation at 68 °C for 30 cycles, and final elongation for 5 minutes at 68 °C. The products were migrated on a 2% agarose gel following the same protocol as the qPCR products, except for the ladder used which was the 1 kb Plus DNA ladder (New England Biolabs).

Supplementary tables

Table S1. Sequence processing throughout analytical pipeline. Amount of filtered water (mL), DNA, RNA and cDNA concentrations (ng/ μ L) (detection limit (ld) of 0.02 ng/ μ L), sequencing yield (read count) and DADA2 processing for DNA read processing only (counts), including the number of filtered reads (truncLen = 280,215; maxN = 0; maxEE = 2,2; truncQ = 2; trimLeft = 17,21), forward (F) and reverse (R) denoised reads, number of merged reads and non-chimeric reads (method “consensus”). Remaining quality-filtered, non-chimeric reads are ASVs.

Sample ID	Filt. water (mL)	DNA (ng/ μ L)	RNA (ng/ μ L)	cDNA (ng/ μ L)	Sequencing yield (counts)	DADA2 pipeline for DNA read processing (counts)				
						filtered	denoised F	denoised R	merged	nonchim (ASV)
SEP_0A	870	4.36	<ld	0.404	47,448	34,303	27,760	32,416	16,882	9,458
SEP_0B	750	23.2	<ld	0.536	39,540	33,162	29,143	31,856	20,063	8,483
SEP_3A	740	3.96	<ld	0.612	50,564	36,521	30,014	34,367	18,018	10,089
SEP_3B	900	5.56	<ld	0.488	38,040	32,545	26,423	30,653	15,875	7,725
SEP_7A	530	8.12	<ld	0.5	52,247	36,729	32,223	35,149	24,612	12,018
SEP_7B	430	10.2	19.8	1.55	30,101	25,238	21,402	23,787	16,136	8,181
SEP_SA	NA	35	164	2	32,412	26,990	13,640	20,966	4,307	4,110
SEP_SB	NA	9.4	99.6	1.83	26,782	22,464	11,620	17,324	3,976	4,636
OCT_0A	1370	11.4	<ld	0.504	25,353	21,771	17,940	20,522	11,011	7,496
OCT_0B	865	3.72	5.34	0.686	49,763	35,931	30,212	34,046	18,952	10,126
OCT_3A	1090	3.34	<ld	0.502	29,203	25,000	20,446	23,439	12,193	7,624
OCT_3B	1020	5.32	5.8	0.748	50,784	36,672	31,002	34,719	18,688	9,579
OCT_7A	1000	5.4	<ld	0.562	49,338	35,143	29,218	33,125	17,795	9,651
OCT_7B	1290	10.7	<ld	1	30,792	26,308	21,318	24,539	12,674	3,463
OCT_SA	NA	24.4	118	2.38	30,486	25,472	13,541	20,031	4,316	2,759
OCT_SB	NA	9.86	79.2	2.09	23,250	19,687	9,937	14,976	3,361	7,597
NOV_IA	1690	1.34	<ld	0.86	47,067	34,682	31,512	33,689	22,462	11,121
NOV_IB	1560	0.728	<ld	<ld	31,819	27,354	25,032	26,587	18,026	6,610

Sample ID	Filt. water (mL)	DNA (ng/μL)	RNA (ng/μL)	cDNA (ng/μL)	Sequencing yield (counts)	DADA2 pipeline for DNA read processing (counts)				
						filtered	denoised F	denoised R	merged	nonchim (ASV)
NOV_0A	1110	7.04	<ld	0.872	44,197	32,345	29,220	31,370	19,217	9,352
NOV_0B	780	12.5	<ld	0.992	27,772	24,225	21,595	23,510	14,388	3,549
NOV_3A	1490	18	5.04	0.73	48,437	35,754	30,007	33,911	17,057	9,370
NOV_3B	660	6.84	<ld	0.948	33,682	29,187	25,161	27,878	14,954	3,431
NOV_7A	2220	2.5	<ld	<ld	49,042	35,416	29,359	33,394	16,244	9,736
NOV_7B	1100	7.26	<ld	0.021	32,726	28,397	23,651	26,829	12,809	7,162
NOV_SA	NA	19.7	104	2.01	30,287	25,555	13,521	19,662	4,412	7,891
NOV_SB	NA	5.8	24.2	1.2	26,241	22,256	11,684	16,941	3,900	7,208
DEC_IA	1480	<ld	<ld	1.08	57,184	43,843	43,026	43,669	39,593	29,114
DEC_IB	1660	0.065	<ld	1.03	37,584	33,414	31,855	32,945	26,856	11,631
DEC_0A	1280	3.52	<ld	1.05	43,421	31,123	27,498	29,797	18,956	11,569
DEC_0B	1590	8.22	<ld	0.876	26,097	22,769	20,104	21,838	13,934	11,147
DEC_3A	1940	6.96	<ld	0.027	48,879	36,051	30,792	34,403	18,798	10,307
DEC_3B	1550	8.96	<ld	1.19	30,794	26,821	22,838	25,376	13,222	16,375
DEC_7A	800	7.8	8.82	0.91	51,534	37,792	30,886	35,166	17,526	9,469
DEC_7B	915	14.2	3.06	1.6	34,620	29,875	23,579	27,563	12,565	10,447
DEC_SA	NA	10.6	57	1.89	33,638	27,824	14,862	21,726	4,586	10,044
DEC_SB	NA	2.26	8.74	0.76	28,504	23,782	12,605	18,471	3,766	13,206
JAN_IA	1660	0.073	<ld	1.1	52,378	39,613	38,519	39,216	33,717	15,683
JAN_IB	1875	0.132	<ld	0.992	34,582	30,324	29,031	29,837	24,471	3,592
JAN_0A	1680	7.92	7.26	0.766	45,135	32,389	27,335	30,627	17,314	10,538
JAN_0B	1400	5.3	<ld	0.02	30,059	26,010	22,139	24,498	13,927	10,402
JAN_3A	1420	7.8	<ld	0.788	47,328	34,457	29,441	32,782	20,430	13,487
JAN_3B	1710	20.6	<ld	0.86	32,854	28,122	24,237	26,915	16,825	3,140
JAN_7A	1060	11.6	1.12	1.03	44,328	32,086	27,251	30,454	17,254	10,935
JAN_7B	1250	11.4	<ld	1.2	31,511	27,204	22,995	25,711	14,557	3,124

Sample ID	Filt. water (mL)	DNA (ng/μL)	RNA (ng/μL)	cDNA (ng/μL)	Sequencing yield (counts)	DADA2 pipeline for DNA read processing (counts)				
						filtered	denoised F	denoised R	merged	nonchim (ASV)
JAN_SA	NA	10.3	136	1.99	27,421	22,981	11,604	17,696	3,669	4,421
JAN_SB	NA	5.54	106	1.27	26,234	21,836	11,556	16,665	3,539	3,397
FEB_IA	1225	0.062	16.2	0.762	48,583	36,826	35,286	36,169	28,324	13,993
FEB_IB	1790	0.064	<ld	0.7	30,352	26,606	24,986	25,963	19,110	11,632
FEB_0A	1495	7.56	<ld	0.952	47,420	34,084	29,429	32,461	19,672	11,598
FEB_0B	1625	7.5	<ld	0.976	20,366	17,522	14,852	16,671	10,265	9,695
FEB_3A	1450	13.8	<ld	0.92	48,018	34,285	29,723	32,762	21,453	14,596
FEB_3B	1720	15.8	<ld	0.992	29,498	25,210	21,552	24,068	15,008	9,569
FEB_7A	1450	31.2	<ld	1.3	47,930	33,977	29,098	32,294	20,512	13,558
FEB_7B	1550	30	<ld	1.06	32,936	28,261	23,656	26,773	15,865	9,888
FEB_SA	NA	9	106	2.06	24,028	20,358	10,071	15,661	3,185	10,386
FEB_SB	NA	6.4	59	1.53	25,016	20,662	10,636	15,978	3,191	10,024
MAR_IA	1350	0.127	<ld	0.952	48,847	36,488	34,566	35,783	26,439	12,157
MAR_IB	1550	0.286	<ld	1.07	27,443	23,856	21,966	23,070	15,308	4,893
MAR_0A	2230	2.84	<ld	0.271	43,154	30,976	26,193	29,296	17,046	10,163
MAR_0B	1905	5.7	<ld	1.05	25,367	21,838	18,103	20,566	11,501	4,265
MAR_3A	1725	1.57	<ld	0.92	45,143	32,409	27,680	30,961	18,323	11,204
MAR_3B	1925	10.6	<ld	0.976	29,072	24,778	20,839	23,468	13,320	7,109
MAR_7A	1070	12.6	<ld	0.892	47,470	33,712	27,251	31,456	15,550	9,624
MAR_7B	1360	29	2.02	1.28	29,424	25,279	20,444	23,617	11,890	4,444
MAR_SA	NA	9.64	44.6	1.6	30,597	25,799	13,984	20,414	4,216	3,629
MAR_SB	NA	2	7.92	0.602	34,255	28,529	14,795	22,184	4,698	3,665
APR_IA	1750	0.124	<ld	0.96	29,488	25,922	24,442	25,275	18,624	13,950
APR_IB	1540	0.094	13.6	0.758	24,032	21,159	19,604	20,567	14,466	14,980
APR_0A	1515	0.524	5.52	0.806	27,690	23,966	21,140	22,946	12,789	11,908
APR_0B	1260	0.636	<ld	1.05	31,201	27,073	23,594	25,770	14,183	10,499

Sample ID	Filt. water (mL)	DNA (ng/μL)	RNA (ng/μL)	cDNA (ng/μL)	Sequencing yield (counts)	DADA2 pipeline for DNA read processing (counts)				
						filtered	denoised F	denoised R	merged	nonchim (ASV)
APR_3A	1670	13.3	0.5	1.2	33,874	28,812	23,768	27,224	13,853	9,906
APR_3B	1455	9.74	<ld	1.03	28,042	24,062	19,741	22,557	10,990	30,314
APR_7A	730	12.7	0.42	1.07	33,354	28,374	17,042	23,368	6,737	12,007
APR_7B	785	42.4	1.2	1.26	27,129	23,213	13,644	18,528	4,947	15,084
APR_SA	NA	4.46	73	1.64	32,281	27,117	14,464	21,604	4,584	11,039
APR_SB	NA	7.78	65	2.03	34,248	28,412	15,149	22,479	4,477	13,935
MAY_1A	2400	0.049	<ld	1.08	34,079	29,662	27,260	28,716	19,057	8,797
MAY_1B	2640	<ld	17.2	1.08	39,913	35,132	34,112	34,849	29,405	12,453
MAY_0A	1315	2.06	1.15	1.19	32,131	27,896	23,285	25,776	14,144	4,311
MAY_0B	1390	2.94	16.4	1.27	25,115	21,967	17,070	19,770	8,963	3,440
MAY_3A	1390	11.1	1.69	1.24	32,203	27,485	21,216	24,919	11,375	3,296
MAY_3B	1050	8.18	6.88	0.802	30,429	26,340	19,448	23,555	8,948	3,701
MAY_7A	750	28.2	<ld	1.1	27,828	24,186	17,175	20,853	8,243	3,361
MAY_7B	680	12.9	<ld	0.884	30,319	26,366	18,551	22,746	9,157	3,653
MAY_SA	NA	8	104	1.99	26,865	22,497	12,137	17,583	3,623	9,518
MAY_SB	NA	4.7	81	2.06	33,732	27,889	14,997	21,870	4,371	9,989
JUN_0A	1360	7.62	9.82	0.694	29,451	25,177	20,455	23,592	11,909	3,121
JUN_0B	1140	11.6	5.5	0.738	27,970	24,051	19,530	22,328	11,202	2,928
JUN_3A	1210	10.2	2.28	1.46	32,944	28,322	23,042	26,458	13,196	3,288
JUN_3B	1160	9.08	12.6	0.766	31,733	27,089	22,016	25,301	12,507	4,192
JUN_7A	1180	10.4	0.614	1.18	33,732	28,975	23,185	26,976	12,984	2,949
JUN_7B	1210	12.4	0.68	1.04	32,558	28,043	22,389	25,858	12,528	3,229
JUN_SA	NA	2.08	77.4	1.45	23,305	12,184	18,086	3,568	4,420	4,420
JUN_SB	NA	1.05	10.2	0.646	19,729	10,065	15,177	2,816	3,945	3,945

Supplementary figures

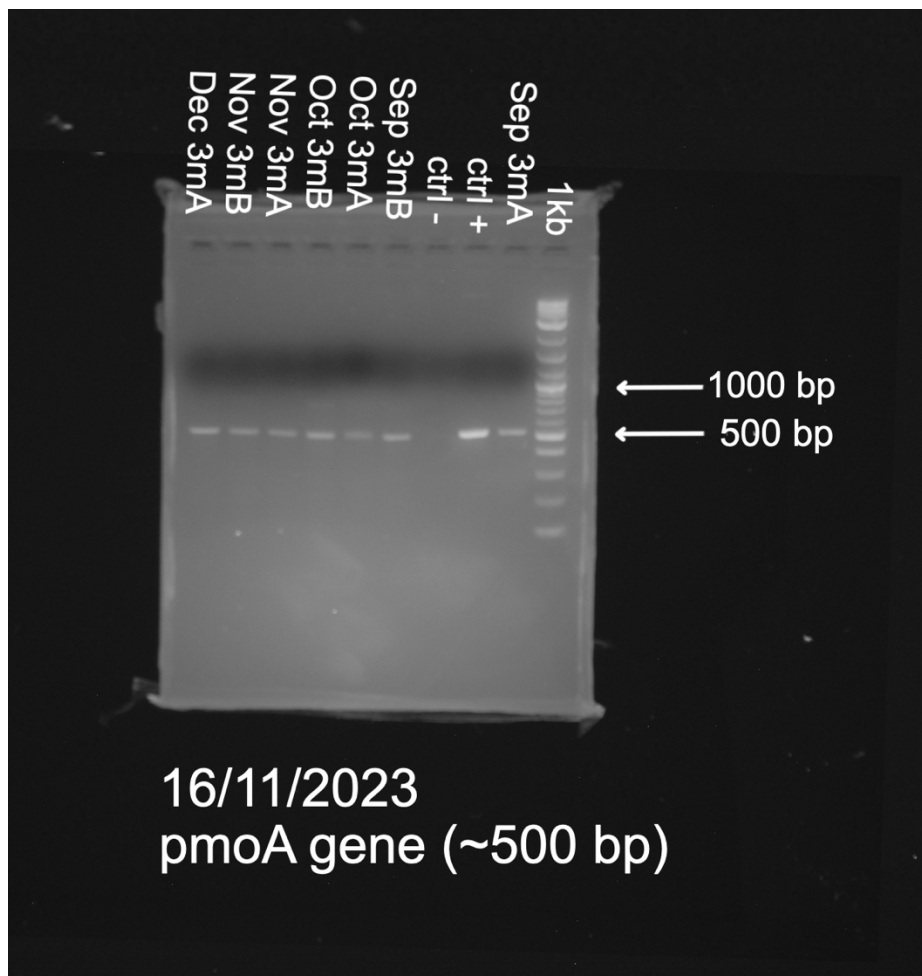


Figure S1. Migration sur gel d'agarose 2% (échelle 1 kb) des produits de PCR pour confirmer l'amplification du gène pmoA avec les amorces A189F et mb661r sur l'ADN. Ctrl signifie contrôle.

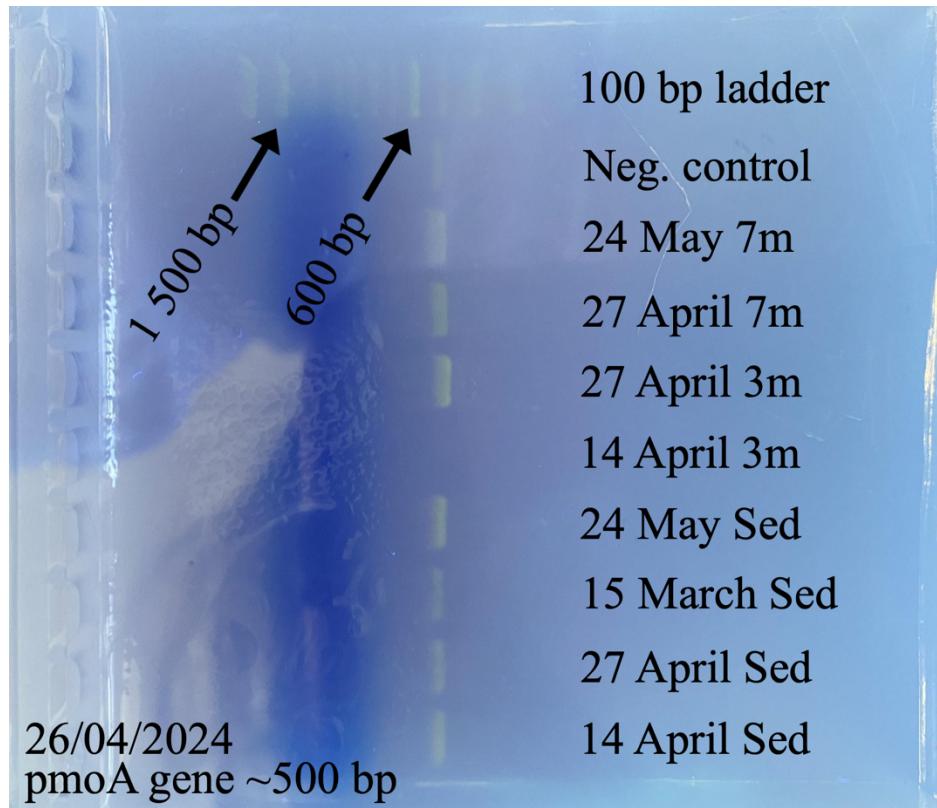


Figure S2. Confirmation de la taille des produits de qPCR (ADNc) provenant des échantillons d'eau et de sédiments, migré sur gel d'agarose 2%

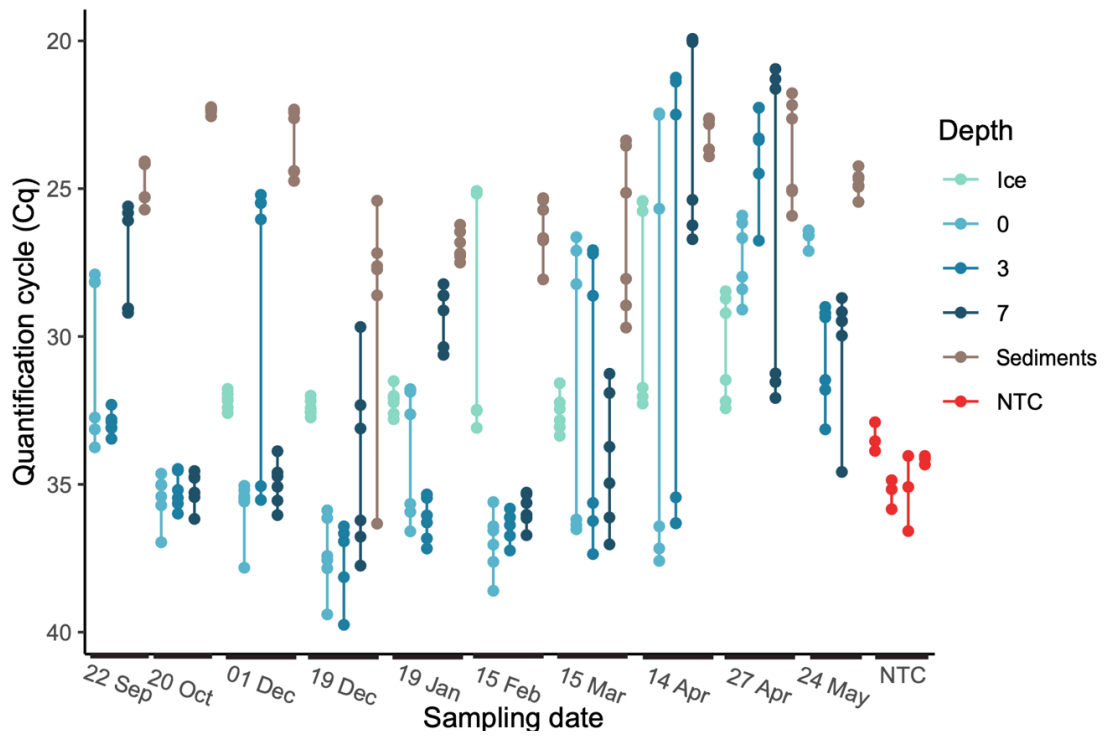


Figure S3. Cycle de quantification (Cq) de tous les échantillons par profondeur à chaque date d'échantillonnage, incluant les NTC (en rouge).

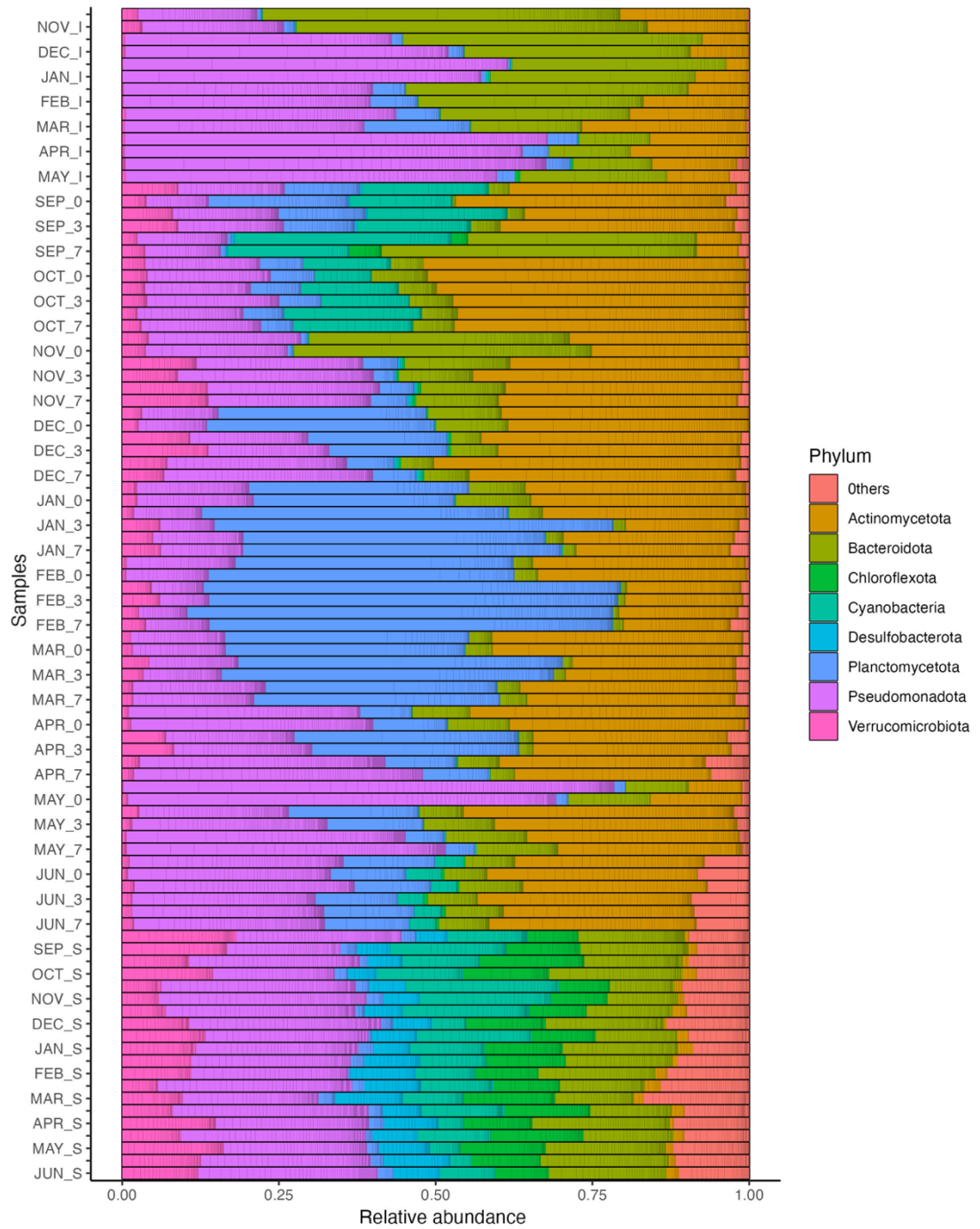


Figure S4. Abondance relative au niveau du phylum dans la glace, l'eau et les sédiments, avec deux répliqués biologiques par échantillon. Les phyla avec une abondance relative inférieure à 1% ont été groupés dans *Others*.